SLAC-PUB-2115
May 1978
(T/E)

THE PRODUCTION OF REAL PHOTONS AT LARGE TRANSVERSE MOMENTUM IN PP COLLISIONS*

R. Rückl
Department of Physics
University of California, Los Angeles, California 90024

and

Max-Planck-Institut für Physik und Astrophysik
München, Federal Republic of Germany

and

S. J. Brodsky
Stanford Linear Accelerator Center
Stanford University, Stanford, California 94305

and

J. F. Gunion†
Department of Physics
University of California, Davis, California 95616

ABSTRACT

The production of photons at large transverse momentum can be used as a direct probe of quark and gluon subprocesses at short distances. We calculate the cross section for high p_T photons produced in pp collisions from lowest order quantum chromodynamics and higher order constituent interchange model processes. We find that CIM terms dominate both γ and π spectra until very high p_T—although there are regions of s and p_T where the CIM contributions dominate the γ spectrum but the π spectrum already shows the scaling behavior of lowest order QCD, and also vice versa. We emphasize that in some processes (e.g., gluon + quark → photon + quark), the photon is produced without accompanying toward side hadrons.

(Submitted to Phys. Rev. D)

---

*Work supported in part by the Department of Energy.
†A.P. Sloan Foundation Fellow

I. INTRODUCTION

Single hadrons and hadronic jets observed at large transverse momenta in hadron collisions seem to originate in hard, large angle scattering processes between constituents of the colliding hadrons.[1] Such subprocesses are, if the parton picture is true, also sources of prompt real photons, i.e. γ's which do not result from π^o, K^o, η etc. decays. Thereby, one can think of two sharply contrasting production mechanisms. High p_T photons could be produced via essentially the same hadronic mechanisms as pions or ρ's. This is the basic assumption of any Vector Meson Dominance Model. The corresponding photon to pion ratio, consequently, would be constant (of order α) apart from a slow s-dependence coming from producing more and more vector mesons as the total center of mass energy $\sqrt{s}$ increases. However, a photon, unlike a color singlet hadron bound state, also has a pointlike coupling to a quark [as evident from scaling in deep inelastic e(μ)-N scattering etc.]. Thus in field theoretic models, such as QCD, the photon can participate much more directly in any given subprocess than a hadron. It is, in fact, the only non-colored elementary field (ignoring weak interactions) that is directly measurable and, therefore, is a critical tool for probing short distance dynamics.[2]

The elementary nature of the photon should become transparent at large transverse momenta. This is most easily seen in the Bjorken-Paschos analysis[2] of deep inelastic Compton scattering $\gamma p \to \gamma X$ where the pointlike photon-quark interaction in the subprocess $\gamma q \to \gamma q$ indeed must dominate the contribution from hadron-like couplings at sufficiently large momentum transfer. We emphasize that even for real photons, the pointlike coupling of the quark current emerges and dominates at large p_T, in parallel to high mass virtual photon reactions. We note that unless $\frac{d\sigma}{dt}(\gamma q \to \gamma q)$ and $\frac{d\sigma}{dt}(eq \to eq)$ have similar

scaling properties at large momentum transfer, it is unlikely that processes like $\frac{d\sigma}{dt}$ $(gq \to gq)$ have canonical point-like behavior. Moreover, the incoming photon transfers all its energy into the large p_T process. No energy is carried away by hadronic spectators.[3]

Photons produced in hadronic collisions reveal their pointlike nature in several ways. Let us consider the quark-gluon subprocess in QCD as an illustration:

(i) The photon can participate directly in the subprocess $gq \to \gamma q$ yielding a p_T^{-4} contribution to the inclusive γ-spectrum. It is produced without any trigger suppression whereas, at the p_T^{-4} level, a pion can only arise indirectly via fragmentation from a quark or gluon scattered into a large angle.

(ii) The photon can also fragment from the scattered quark in $gq \to gq(q \to \gamma)$ (bremsstrahlung). In this case, its pointlike coupling is reflected in the difference of the fragmentation functions[4] (Figure 1):

$$D_{\gamma/q} \sim \frac{(1-x)^0}{x} \qquad \text{versus} \qquad D_{\pi/q} \sim \frac{(1-x)^{1 \text{ or } 2}}{x} \ .$$

The stronger power suppression of pions with a large fraction x of the quark momentum is a direct consequence of the composite nature of the pion.

Altogether it is obvious that γ/π is not expected to be constant even at the purely QCD - p_T^{-4} level. In fact $\frac{\gamma}{\pi} \to \infty$ as $\epsilon = 1-x_T$ $(x_T = \frac{2p_T}{\sqrt{s}})$ approaches 0 at fixed θ_{cm} for both (i) and (ii).

In addition, there are contributions from constituent interchange processes to both γ and π production. They yield inclusive spectra which fall off more rapidly with p_T but may still dominate the above QCD contributions at moderate p_T. Here the elementary nature of the photon is especially apparent causing different p_T-behavior of the leading contributions to γ and π :[5]

(a) The γ-production in pp-collisions in the CIM is dominated by $Mq \to \gamma q$ yielding

$$E \frac{d\sigma}{d^3p} (pp \to \gamma) \sim \frac{\varepsilon^9}{p_T^6} \quad \text{and}$$

(b) the π-production is dominated by $Mq \to \pi q$ yielding

$$E \frac{d\sigma}{d^3p} (pp \to \pi) \sim \frac{\varepsilon^9}{p_T^8} \quad ,$$

where M is a meson-like $q\bar{q}$-component in the proton wave function. So, $\frac{\gamma}{\pi}$ grows as p_T^2 at fixed θ_{cm}. We discuss the normalization of these processes in Section IV.

There is already evidence from several experiments that the photon has to be treated, at least partly, as a fundamental field. For example, if it were dominantly a $q\bar{q}$ bound state, all of the following ratios would be constant:

(1) SLAC[6] ($\theta_{cm} = 90°$, $E_\gamma^{lab} = 4,5,7.5$ GeV):

$$\frac{\frac{d\sigma}{dt} (\gamma p \to \pi^+ n)}{\frac{d\sigma}{dt} (\pi^+ p \to \pi^+ p)} \sim s^{0.3 \text{ to } 0.7} \quad ;$$

(2) CORNELL[7] ($\theta_{cm} = 90°$, $E_\gamma^{lab} = 3$ to 6 GeV):

$$\frac{\frac{d\sigma}{dt} (\gamma p \to \gamma p)}{\frac{d\sigma}{dt} (\gamma p \to \pi^o p)} \sim s^{2.1 \pm 0.6} \quad ;$$

(3) SLAC[8] (21 GeV bremsstrahlung, $p_T = 1$ to 1.7 GeV/c, $0 \leq \varepsilon \leq 0.4$):

$$\frac{E \frac{d\sigma}{d^3p} (\gamma p \to \gamma X)}{E \frac{d\sigma}{d^3p} (\gamma p \to \pi X)} \sim p_T^{2.6 \text{ to } 6.2} \quad ;$$

(4) ISR[9] ($\theta_{cm} = 90°$, $\sqrt{s} = 45{,}53$ GeV):

$$\frac{E\frac{d\sigma}{d^3p}(pp \to \gamma X)}{E\frac{d\sigma}{d^3p}(pp \to \pi X)} \sim \begin{cases} 15\% \text{ at } p_T \sim 3 \text{ GeV/c} \\ 25\% \text{ at } p_T \sim 3.7 \text{ GeV/c} \end{cases}$$

To test the picture of γ-production sketched above, far more data are needed, preferably at higher energies and/or larger p_T. Here we would like to draw attention to some of its consequences which do not depend critically on our numerical analysis. A unique signature of the pointlike photon-quark coupling is the production of high p_T photons in $gq \to \gamma q$ and $Mq \to \gamma q$ without accompanying hadrons in the jet (apart from the usual low p_T background). In contrast, a hadron at high p_T is generally accompanied by other fragments of its source (quark or gluon at the p_T^{-4} - level, or resonance at the p_T^{-8} - level). A hadron veto at the trigger side would remove the fragmentation component in the γ-spectrum [e.g. from process (ii)] and display the special role of the photon explicitly. We urge such an experiment to be done. Since the two prompt subprocesses (i) and (a) are in fact the dominant γ sources,[10] there is another remarkable consequence. The photon is nearly always balanced by an opposite side quark jet, whereas a pion can arise from a fragmentation of the scattered quark in $gq \to gq$ with the balancing jet being a gluon. Finally we note that the balance among contributing quarks shifts in going from pions to photons. The photon emphasizes the u quark components of the colliding hadrons, whereas a π^o, for example, sees u and d quarks equally. Thus, if the γ is a fragment of a quark, one should observe a hadron asymmetry among the accompanying hadrons in the jet in favor of hadrons containing a u quark, e.g. $\pi^+ > \pi^-$. Similarly, π^+'s will be more effective in producing high p_T γ's than will π^-'s.

In the following sections we present a complete description of the inclusive production of real photons in pp-collisions from moderate up to very high p_T. For definiteness, we choose $\theta_{cm} = 90°$. The paper is organized as follows:

Section II: Brief description of the technique used in our calculations, discussion of general features of γ to π and γ to jet ratios and some remarks on gauge invariance.

Section III: Derivation and summary of the results for γ and π production from lowest order QCD-subprocesses (p_T^{-4} - contributions).

Section IV: Investigation of higher order (Constituent Interchange Model) processes, the significant contributions of which yield p_T^{-6} - terms for the γ-spectrum and p_T^{-8} - terms for the π-spectrum.

Section V: Discussion of our predictions and conclusions. We find that CIM terms dominate both γ and π - spectra at moderate p_T, while the p_T^{-4} - terms become dominant at very high p_T. Because of the different p_T-behavior of the CIM contributions to γ and π production, there are also regions where CIM still dominates the γ-spectrum but the π-spectrum already shows the typical p_T^{-4} - behavior of lowest order QCD or vice versa.

The quark fragmentation function into a photon is discussed in Appendix A on the basis of pure QED bremsstrahlung. In Appendix B we demonstrate how the pointlike nature of the photon leads to a harder p_T-spectrum than the one of a composite hadron in the framework of a ϕ^3-theory.

The absolute normalization of our subprocesses is consistent with the available experimental information and various theoretical arguments. Nevertheless, at this point there is inevitably some numerical uncertainty in our results. We, therefore, give all cross sections explicitly in terms of the occurring coupling constants.

II. FORMALISM AND SOME GENERAL REMARKS

The formalism and most of the parameters used in our calculations later on are described in detail in references 5 and 11. We will, therefore, only give a brief summary.

The basic picture we adopt is that a single particle (here π's or γ) or a jet at high transverse momentum has its origin in hard scattering subprocesses between constituents (quarks, gluons, mesonic $q\bar{q}$ or baryonic qqq components) of the colliding hadrons (A and B). The observed particle can either participate in the process in which the large momentum transfer occurs ("prompt process") or be produced afterwards via fragmentation from a scattered constituent ("final bremsstrahlung").

Suppose the cross section for the subprocess ab $\to$ cd at large momentum transfer is given by

$$\frac{d\sigma}{dt}(ab \to cd) = \frac{\pi \mathcal{D}}{s^{N-T-U}\,(-t)^{T}\,(-u)^{U}} \quad , \tag{2.1}$$

where $\mathcal{D}$ contains the relevant coupling constants. The cross section for AB $\to$ c follows, then, simply by folding (2.1) with the probabilities $G_{a/A}(x_a)[G_{b/B}(x_b)]$ for finding a constituent of type a(b) inside A(B) carrying the light cone fraction $x_a = \dfrac{p_a^o + p_a^3}{p_A^o + p_A^3}$ $\left(x_b = \dfrac{p_b^o - p_b^3}{p_B^o - p_B^3}\right)$ of the incident momentum.

We will use a simple form for these distribution functions suggested by dimensional counting:

$$\begin{aligned} x\,G_{a/A}(x) &= (1+g_a) f_{a/A}\, N(a/A)(1-x)^{g_a} \qquad x > \hat{x}_a \\ &= (1+g_a) f_{a/A}\, N(a/A)(1-\hat{x}_a)^{g_a} \qquad x > \hat{x}_a \quad . \end{aligned} \tag{2.2}$$

The parameters

g_a: 2 × (minimum number of quarks in the spectator system) - 1 ;

$f_{a/A}$: fraction of total momentum of A carried by a ;

N(a/A): shape factor, controlling the transition from the (1-x) - power behavior in the valence region to the Regge behavior in the sea region; and

$\hat{x}_a$: value of x at which this transition starts

are discussed in references 5 and 11 and for protons listed in Table I for various constituents. The integrations are elementary and one finds for $\theta_{cm} = 90°$ and large enough $x_T [x_T \gtrsim \frac{1}{2}(\hat{x}_a+\hat{x}_b)]$:

$$E \frac{d\sigma}{d^3p} (AB \to c) = I \frac{\varepsilon^F}{p_T^{2N}} \tag{2.3}$$

with $\varepsilon = 1-x_T$, $x_T = \frac{2p_T}{\sqrt{s}}$ and p_T the transverse c momentum, $F = 1+g_a+g_b$ and

$$I = \mathcal{D} \sum_{\substack{a\in A \\ b\in B \\ \text{color}}} f_{a/A}\, N(a/A)\, f_{b/B}\, N(b/B)\, 2^{2+g_a+g_b+T+U-2N} \frac{\Gamma(2+g_a)\,\Gamma(2+g_b)}{\Gamma(2+g_a+g_b)} . \tag{2.4}$$

In case of a prompt process, c itself is the trigger particle and (2.3) the corresponding inclusive cross section. If the observed particle, however, results from a fragmentation of c we, further, have to integrate (2.3) over the probability $D_{C/c}(w)$ that C fragments from c with a light cone fraction w of the momentum of c. Again we use a simple power law[11]

$$w\, D_{C/c}(w) = d_{C/c}(1-w)^{g_{C/c}} . \tag{2.5}$$

The parameters for $C = \pi^{\pm}$ and $c = q$ or $\bar{q}$ are given in Table II and provide a reasonable description of e^+e^- - data. The gluon decay parameters are discussed in reference 11.

TABLE I: Structure Function Parameters (per color) of a Proton

a	g_a	$f_{a/p}$	N(a/p)	$\hat{x}_a$
u	3	0.1	1.2	0.2
d	3	0.067	1.2	0.2
$\bar{q}$	7	0.01	1	0
g	4	0.063	1	0
M	5	0.1	2.4	0.3
B	3	0.12	1.6	0.3

TABLE II: Fragmentation Function Parameters for $\pi^{\pm}$ †

$c \to \pi^+$	$g_{\pi/c}$	$d_{\pi/c}$	$c \to \pi^-$
u	1	0.5	$\bar{u}$
$\bar{d}$	1	0.5	d
d	5	0.5	$\bar{d}$
$\bar{u}$	5	0.5	u
g	2	0.5	g

†We use dimensional counting for the disfavored mesons (i.e. g=5). Resonance contributions may be important resulting in g=2. This, however, has a small effect on the π production result quoted.

In Appendix A we show that the effective[12] fragmentation function for a photon from a quark can be characterized by

$$g_{\gamma/q} = 0 \qquad \text{and} \qquad d_{\gamma/q} = \frac{1}{\pi}\lambda_q^2 \alpha_\gamma \quad . \tag{2.6}$$

λ_q is the quark charge in units of the electron charge and α_γ is an effective coupling constant: $\alpha^\gamma \simeq \alpha \ln \eta$ where α is the fine structure constant and $\eta \sim \frac{\sqrt{s}}{m_q}$. Numerically we will take $\ln \eta \sim 4$. From (2.3) and (2.5) we finally get for a fragmentation component in the inclusive spectrum:

$$E\frac{d\sigma}{d^3p}(AB \to c \to C) = d_{C/c}\frac{\Gamma(g_{C/c}+1)\,\Gamma(F+1)}{\Gamma(g_{C/c}+F+2)}\kappa(g_{C/c},F,N)\; I\,\frac{\varepsilon^{F+g_{C/c}+1}}{p_T^{2N}} \quad .$$

$$\text{with} \quad \kappa(g,F,N) = \left(1 - \frac{g}{g+F}\varepsilon\right)^{2N-F-3} \quad . \tag{2.7}$$

All cross sections in this paper are calculated employing formulas (2.3) and (2.7).

A quick glance at these results shows an interesting feature common to all models with quark jets. The $\frac{\gamma}{\text{jet}}$ and $\frac{\gamma}{\pi}$ ratios for photons and pions produced via fragmentation from a q-quark jet in a given subprocess are roughly universal, namely

$$\frac{\gamma}{\text{jet}} = \frac{d_{\gamma/q}}{F+1}\varepsilon \quad \text{and} \tag{2.8}$$

$$\frac{\gamma}{\pi} = \frac{d_{\gamma/q}}{d_{\pi/q}}\frac{F+2}{\kappa(1,F,N)}\frac{1}{\varepsilon} \quad . \tag{2.9}$$

We have defined the theoretical jet cross section to be the cross section for production of a quark (or gluon) of given p_T. The particular dynamics of the subprocess only enters via the N dependence of $\kappa(1,F,N)$ in the denominator of (2.9), which is, however, very weak since $\frac{g}{g+F}\varepsilon << 1$ [see (2.7) and Tables I and II]. Otherwise, these ratios are determined exclusively by structure

and fragmentation function parameters. Numerically, if we have equal numbers of u and d quark jets, then for F~10

$$\frac{\gamma}{\text{jet}} \simeq \frac{1}{2}\frac{\alpha_\gamma\left(\frac{4}{9}+\frac{1}{9}\right)}{11\pi}\varepsilon \simeq 0.008\,\alpha_\gamma\,\varepsilon \simeq 2\times10^{-4}\varepsilon$$

$$\frac{\gamma}{\pi^o} \simeq \frac{\alpha_\gamma\left(\frac{4}{9}+\frac{1}{9}\right)12}{0.5\pi}\frac{1}{\varepsilon} \simeq \frac{4.24\alpha_\gamma}{\varepsilon} \simeq \frac{0.12}{\varepsilon} \quad . \tag{2.10}$$

In a more detailed calculation such as that appropriate to the "old" Feynman-Field model,[1] which contains quark jets only, we find (see Appendix B)

$$\frac{\gamma}{\text{jet}} \sim 4\times10^{-4} \quad \text{and} \quad \frac{\gamma}{\pi^o} \sim 17\% \tag{2.11}$$

at ISR energy, $\sqrt{s} \sim 53$ GeV and $p_T \sim 6$ GeV/c, $\varepsilon \sim 0.77$. Note that $\frac{\gamma}{\pi} \sim \left(\frac{F}{\varepsilon}\right)^2 \frac{\gamma}{\text{jet}} >> \frac{\gamma}{\text{jet}}$, clearly due to the pointlike γ-q coupling. To summarize our analysis of quark jet fragmentation, we have[13]

$$\frac{\pi}{\text{jet}} \sim \left(\frac{\varepsilon}{F}\right)^2 \quad , \quad \frac{\gamma}{\text{jet}} \sim \alpha\left(\frac{\varepsilon}{F}\right) \quad ,$$
$$\text{and} \quad \frac{\gamma}{\pi} \sim \alpha\left(\frac{F}{\varepsilon}\right) \quad . \tag{2.12}$$

It might be interesting to mention that the situation is different in electron-positron annihilation.[14] There, the production cross sections of π and γ are directly proportional to the corresponding fragmentation functions,

$$\frac{1}{\sigma}\frac{d\sigma}{dx}(e^+e^- \to \pi^o) = \frac{2\sum_{q=u,d}\lambda_q^2 D_{\pi^o/q}(x)}{\sum_{q=u,d,s,c}\lambda_q^2} \tag{2.13}$$

$$\frac{1}{\sigma}\frac{d\sigma}{dx}(e^+e^- \to \gamma) = \frac{2\sum_{q=u,d,s,c}\lambda_q^2 D_{\gamma/q}(x)}{\sum_{q=u,d,s,c}\lambda_q^2}$$

with $x = \frac{p}{p_{max}}$. Consequently, for $\varepsilon = 1-x \to 0$

$$\frac{\gamma}{\pi^o} = \frac{2\alpha_\gamma \sum_{q=u,d,s,c}\lambda_q^4}{\pi\, d_{\pi^+/u}\,(\lambda_u^2+\lambda_d^2)}\frac{1}{\varepsilon} = \frac{0.96\alpha_\gamma}{\varepsilon} \simeq \frac{0.028}{\varepsilon}\,, \qquad (2.14)$$

that is about a factor of 5 smaller than in pp-collisions, since the factor F is absent.

In the following, the subprocesses yielding high p_T photons will be classified into prompt processes and final bremsstrahlung processes as discussed in the Introduction [(i) and (ii)]. The latter class alone is certainly not gauge invariant. We want to show here how gauge invariance is restored for γ production in $q'q \to q'q\gamma$. The argumentation is, in principle, the same for other bremsstrahlung processes. Further, we only consider the radiation from one quark (q), since at high energies the radiation from q and q' practically does not interfere. The gauge invariant amplitude is, then, given by the sum of diagram (a) and (b) in Figure 2. The photon spectrum follows from the corresponding cross section by integration over the remaining quark variables, e.g. momentum transfer t and invariant mass M_a^2 (see Figure 2). In the Coulomb gauge and for hard photons at large angles in the center of mass system, one finds for the contributions from the different regions in t:

(1) $\underline{|t| \sim \frac{s}{2}}$: The cross section is dominated by final bremsstrahlung (a) with M_a^2 near the mass shell (note that M_b^2 is always large). In other words, the photon comes off with a small angle with respect to the radiating

quark which itself was scattered into a large angle with respect to the initial quark direction [Figure 3(a)]. Thus final bremsstrahlung resembles a fragmentation from a quark subsequent to the hard scattering process $q'q \to q'q$.

(2) $|t| \ll s$: In this case, kinematics requires both M_a^2 and M_b^2 to be large so that both diagrams (a) and (b) are equally important. But in contrast to (1), q' does not participate directly in the part of the process in which the large momentum transfer takes place. It only radiates a gluon in the very forward direction [Figure 3(b)] . We, therefore, absorb it in the wave function of the initial hadron and, instead, consider $qg \to q\gamma$ the relevant hard scattering process. This shifted subprocess belongs to the class of prompt processes [see Figure 4B] .

(3) $|t| \sim s$: As in (2) M_a^2 and M_b^2 are large and the contributions from (a) and (b) are, therefore, of the same size, but relatively small due to the large momentum transfer. We neglect the contribution from this region. Thus we expect the cross sections for prompt processes and final bremsstrahlung processes together to be gauge invariant.

III. p_T^{-4} - QCD CONTRIBUTIONS

In this section we derive the high p_T photon yield from lowest order QCD subprocesses. Figure 4 shows the Feynman diagrams for the sources we want to consider, separated into final bremsstrahlung (A) and prompt (B) processes. The corresponding non-radiative jet cross sections $pp \to$ single q or $\bar{q}$ or g and inclusive π spectra have been calculated in several papers. We will use the results given in reference 11. Further, we are neglecting s or $\bar{s}$ production whose contribution is small to both pions and photons. Whenever we substitute numerical values for the quark-gluon coupling constant α_s and the quark-photon coupling constant α_γ, we take[15]

$$\alpha_s = 0.15 \quad \text{and} \quad \alpha_\gamma = 4\alpha = \frac{4}{137} \; . \tag{3.1}$$

A. Final Bremsstrahlung

Applying the formalism outlined in the last section, in particular (2.3), (2.6) and (2.7), we find:

(a) $qq \to qq$ $(q \to \gamma)$:

$$E\frac{d\sigma}{d^3p}(pp \to u,d) = \frac{\varepsilon^7}{p_T^4}\alpha_s^2 \times [1.53,\ 1.09]$$

and, therefore,

$$E\frac{d\sigma}{d^3p}(pp \to \gamma) = \frac{\alpha_\gamma}{\pi}\ \frac{1}{8}\ \left(1.53 \times \frac{4}{9} + 1.09 \times \frac{1}{9}\right) \times \alpha_s^2 \frac{\varepsilon^8}{p_T^4}$$

$$= 3.2 \times 10^{-2}\, \alpha_\gamma\, \alpha_s^2 \frac{\varepsilon^8}{p_T^4} \quad ; \tag{3.2}$$

(b) $gq \to gq \ (q \to \gamma)$

$$E\frac{d\sigma}{d^3p}(pp \to u,d) = \frac{\varepsilon^8}{p_T^4}\alpha_s^2 \times [5.11,\ 3.44]$$

and

$$E\frac{d\sigma}{d^3p}(pp \to \gamma) = \frac{\alpha_\gamma}{\pi}\ \frac{1}{9}\ \left(5.11 \times \frac{4}{9} + 3.44 \times \frac{1}{9}\right) \times \alpha_s^2 \frac{\varepsilon^9}{p_T^4}$$

$$= 9.4 \times 10^{-2}\ \alpha_\gamma\ \alpha_s^2 \frac{\varepsilon^9}{p_T^4}\ ; \qquad (3.3)$$

(c) $gg \to q\bar{q} \ (q,\bar{q} \to \gamma)$

$$E\frac{d\sigma}{d^3p}(pp \to u,\bar{u},d,\bar{d}) = \frac{\varepsilon^9}{p_T^4}\alpha_s^2\ \ 0.092 \times [1,1,1,1]$$

and

$$E\frac{d\sigma}{d^3p}(pp \to \gamma) = \frac{\alpha_\gamma}{\pi}\ \frac{1}{10}\ \left(2 \times \frac{4}{9} + 2 \times \frac{1}{9}\right)\ \ 0.092 \times \alpha_s^2 \frac{\varepsilon^{10}}{p_T^4}$$

$$= 3.3 \times 10^{-3}\ \alpha_\gamma\ \alpha_s^2 \frac{\varepsilon^{10}}{p_T^4}\ ; \qquad (3.4)$$

(d) $q\bar{q} \to q\bar{q} \ (q,\bar{q} \to \gamma)$

$$E\frac{d\sigma}{d^3p}(pp \to u,\bar{u},d,\bar{d}) = \frac{\varepsilon^{11}}{p_T^4}\alpha_s^2 \times [1.28,0.57,0.88,0.57]$$

and

$$E\frac{d\sigma}{d^3p}(pp \to \gamma) = \frac{\alpha_\gamma}{\pi}\ \frac{1}{12}\ \left(1.85 \times \frac{4}{9} + 1.45 \times \frac{1}{9}\right) \times \alpha_s^2 \frac{\varepsilon^{12}}{p_T^4}$$

$$= 2.6 \times 10^{-2}\ \alpha_\gamma\ \alpha_s^2 \frac{\varepsilon^{12}}{p_T^4}\ ; \qquad (3.5)$$

(e) $g\bar{q} \to g\bar{q}$ $(\bar{q} \to \gamma)$

$$E\frac{d\sigma}{d^3p}(pp \to \bar{u},\bar{d}) = \frac{\varepsilon^{12}}{p_T^4}\alpha_s^2 \quad 0.95 \times [1,1]$$

and

$$E\frac{d\sigma}{d^3p}(pp \to \gamma) = \frac{\alpha_\gamma}{\pi}\frac{1}{13}\left(\frac{4}{9}+\frac{1}{9}\right) \quad 0.95 \times \alpha_s^2\frac{\varepsilon^{13}}{p_T^4}$$

$$= 1.3 \times 10^{-2}\,\alpha_\gamma\,\alpha_s^2\frac{\varepsilon^{13}}{p_T^4} \quad . \tag{3.6}$$

These results, together with the corresponding quark jet and π^+ spectra (taken from reference 11) are summarized in Table III. Also shown are the resulting $\frac{\gamma}{\pi^+}$ ratios. They should be compared with the general formula (2.9).

B. Prompt Processes

The cross sections (2.1) for the subprocesses (a) - (c) of Figure 4B are obtained from the equivalent QED cross sections (Compton scattering and $e^+e^- \to \gamma\gamma$) by changing one α to $\alpha\lambda_q^2$, the second one to $\frac{\alpha_s}{2}$ and multiplication by the appropriate color factors (average over initial and sum over final color). Their contributions to $pp \to \gamma$ follow, then from (2.3) and (2.4).

(a) $gq \to \gamma q$:

$$\frac{d\sigma}{dt}(gq \to \gamma q) = \frac{2\pi\,\alpha\lambda_q^2\frac{\alpha_s}{2}}{s^2}\frac{s^2+u^2}{-su}\frac{1}{3}$$

TABLE III. Cross sections for the production of quark jets and subsequent fragmentation into γ or π^+ at the QCD-p_T^{-4} level.[16]

subprocess	q-jet	γ	π^+	$\gamma/\pi^+(\alpha_\gamma = 0.029)$
$qq \to qq$	$2.62\ \alpha_s^2\ \frac{\varepsilon^7}{p_T^4}$	$3.2\times10^{-2}\ \alpha_\gamma\ \alpha_s^2\ \frac{\varepsilon^8}{p_T^4}$	$\frac{1.1\times10^{-2}}{\left(1-\frac{\varepsilon}{8}\right)^6}\ \alpha_s^2\ \frac{\varepsilon^9}{p_T^4}$	$8.5\%\ \frac{\left(1-\frac{\varepsilon}{8}\right)^6}{\varepsilon}$
$gq \to gq$	$8.55\ \alpha_s^2\ \frac{\varepsilon^8}{p_T^4}$	$9.4\times10^{-2}\ \alpha_\gamma\ \alpha_s^2\ \frac{\varepsilon^9}{p_T^4}$	$\frac{2.8\times10^{-2}}{\left(1-\frac{\varepsilon}{9}\right)^7}\ \alpha_s^2\ \frac{\varepsilon^{10}}{p_T^4}$	$10\%\ \frac{\left(1-\frac{\varepsilon}{9}\right)^7}{\varepsilon}$
$gg \to q\bar{q}$	$0.37\ \alpha_s^2\ \frac{\varepsilon^9}{p_T^4}$	$3.3\times10^{-3}\ \alpha_\gamma\ \alpha_s^2\ \frac{\varepsilon^{10}}{p_T^4}$	$\frac{8.5\times10^{-4}}{\left(1-\frac{\varepsilon}{10}\right)^8}\ \alpha_s^2\ \frac{\varepsilon^{11}}{p_T^4}$	$11\%\ \frac{\left(1-\frac{\varepsilon}{10}\right)^8}{\varepsilon}$
$q\bar{q} \to q\bar{q}$	$3.3\ \alpha_s^2\ \frac{\varepsilon^{11}}{p_T^4}$	$2.6\times10^{-2}\ \alpha_\gamma\ \alpha_s^2\ \frac{\varepsilon^{12}}{p_T^4}$	$\frac{5.9\times10^{-3}}{\left(1-\frac{\varepsilon}{12}\right)^{10}}\ \alpha_s^2\ \frac{\varepsilon^{13}}{p_T^4}$	$13\%\ \frac{\left(1-\frac{\varepsilon}{12}\right)^{10}}{\varepsilon}$
$g\bar{q} \to g\bar{q}$	$1.9\ \alpha_s^2\ \frac{\varepsilon^{12}}{p_T^4}$	$1.3\times10^{-2}\ \alpha_\gamma\ \alpha_s^2\ \frac{\varepsilon^{13}}{p_T^4}$	$\frac{2.6\times10^{-3}}{\left(1-\frac{\varepsilon}{13}\right)^{11}}\ \alpha_s^2\ \frac{\varepsilon^{14}}{p_T^4}$	$14.5\%\ \frac{\left(1-\frac{\varepsilon}{13}\right)^{11}}{\varepsilon}$

and, therefore,

$$E\frac{d\sigma}{d^3p}(pp \to \gamma) = I\frac{\varepsilon^8}{p_T^4}$$

$$\text{with} \quad I = 2\frac{\alpha\alpha_s}{3}\sum_{\substack{g\epsilon p_A \\ q\epsilon p_B \\ \text{color}}}[f_{g/p}N(g/p)][\lambda_q^2 f_{q/p}N(q/p)][2^6+2^4]\frac{\Gamma(5)\,\Gamma(6)}{\Gamma(9)} \quad .$$

Taking

$$\sum_{\substack{g\epsilon p \\ \text{color}}} f_{g/p}N(g/p) = 8 \times 0.063 = 0.5 \qquad \text{and}$$

$$\sum_{\substack{q\epsilon p \\ \text{color}}} \lambda_q^2 f_{q/p}N(q/p) = 1.2\left(\frac{4}{9}\times 0.3 + \frac{1}{9}\times 0.2\right) \simeq 0.19$$

as resulting from Table I, we estimate:

$$E\frac{d\sigma}{d^3p}(pp \to \gamma) = 0.36\,\alpha\alpha_s\frac{\varepsilon^8}{p_T^4} \quad . \tag{3.7}$$

(b) $q\bar{q} \to g\gamma$:

This cross section follows from (a) by s-t crossing and multiplication by $\frac{8}{3}$ to correct the color average in the initial state:

$$\frac{d\sigma}{dt}(q\bar{q} \to q\gamma) = \frac{2\pi\,\alpha\lambda_q^2\frac{\alpha_s}{2}}{s^2}\frac{t^2+u^2}{tu}\frac{8}{9} \quad .$$

Then,

$$E\frac{d\sigma}{d^3p}(pp \to \gamma) = I\frac{\varepsilon^{11}}{p_T^4} \tag{3.8}$$

with

$$I = 2\frac{8\alpha\alpha_s}{9}\left(\frac{4}{9}\times 0.3\times 0.03+\frac{1}{9}\times 0.2\times 0.03\right) 1.2\,(2^8+2^8)\,\frac{\Gamma(5)\,\Gamma(9)}{\Gamma(12)}$$

$$= 0.12\,\alpha\alpha_s \quad .$$

(c) $g\bar{q} \to \gamma\bar{q}$:

Replacing in (a) the q-parameters by the corresponding $\bar{q}$-parameters, we get:

$$E\frac{d\sigma}{d^3p}(pp\to\gamma) = I\frac{\varepsilon^{12}}{p_T^4} \tag{3.9}$$

$$\text{with}\quad I = 2\,\frac{\alpha\alpha_s}{3}\,0.5\left(\frac{4}{9}+\frac{1}{9}\right)0.03\,(2^{10}+2^8)\,\frac{\Gamma(6)\,\Gamma(9)}{\Gamma(13)}$$

$$= 0.07\,\alpha\alpha_s\,\frac{\varepsilon^{12}}{p_T^4} \quad .$$

In total we have

$$E\frac{d\sigma}{d^3p}(pp\to\gamma x) \cong \frac{\varepsilon^8}{p_T^4}\alpha_s^2\,\alpha_\gamma(3.2+9.4\varepsilon+0.33\varepsilon^2+2.6\varepsilon^4+1.3\varepsilon^5)\times 10^{-2}$$

$$+\frac{\varepsilon^8}{p_T^4}\alpha_s\alpha(0.36+0.12\varepsilon^3+0.07\varepsilon^4)$$

$$\equiv \frac{\varepsilon^8}{p_T^4}\alpha_s^2\,\alpha_\gamma\,F_{BR}^{\gamma}(\varepsilon)+\frac{\varepsilon^8}{p_T^4}\alpha_s\alpha\,F_{PR}^{\gamma}(\varepsilon) \quad . \tag{3.10}$$

Taking for the coupling constants the values (3.1) we see that the dominant contribution comes from the prompt process $qg \to \gamma q$. We emphasize again that the prompt process can be distinguished from the QCD bremsstrahlung contribution by the absence of hadrons on the trigger side (see Introduction).

Finally, the $\frac{\gamma}{\pi^+}$ ratio calculated from all p_T^{-4} QCD sources is given by

$$\left(\frac{\gamma}{\pi^+}\right)_{QCD} \equiv R^{QCD}_{\gamma/\pi}\,\frac{1}{\varepsilon} \tag{3.11}$$

with

$$R^{QCD}_{\gamma/\pi} \cong \frac{\alpha_\gamma\, F^\gamma_{BR}(\varepsilon) + \frac{\alpha}{\alpha_s}\, F^\gamma_{PR}(\varepsilon)}{F^\pi_{QCD}(\varepsilon)} \tag{3.12}$$

F^γ_{BR} and F^γ_{PR} are defined in equation (3.10) and

$$F^\pi_{QCD}(\varepsilon) = \frac{1.1\times10^{-2}}{\left(1-\frac{\varepsilon}{8}\right)^6} + \frac{2.8\times10^{-2}}{\left(1-\frac{\varepsilon}{9}\right)^7}\,\varepsilon + \frac{8.6\times10^{-3}}{\left(1-\frac{\varepsilon}{5}\right)^7}\,\varepsilon^2 + \frac{1.5\times10^{-2}}{\left(1-\frac{2\varepsilon}{11}\right)^8}\,\varepsilon^3 \tag{3.13}$$

In (3.13) we have kept only the four dominant contributions to π^+ production from $qq \to qq(q \to \pi^+)$, $qg \to qg(q \to \pi^+)$, $qg \to qg(g \to \pi^+)$ and $gg \to gg(g \to \pi^+)$, respectively. The gluon fragmentation function is assumed to be of the form given in Table II. Further details may be found in reference 11. We note that, if present, scaling violations from higher order QCD asymptotic freedom corrections tend to cancel in the $\frac{\gamma}{\pi}$ ratio. Thus equation (3.12) should be a reliable prediction of QCD.

Choosing $\alpha_s = 0.15$ this gives

$$\left(\frac{\gamma}{\pi^+}\right)_{QCD} \simeq \begin{cases} 0.4 & \text{at} \quad \varepsilon = 1-x_T = 0.7 \\ 2.5 & \text{at} \quad \varepsilon = 1-x_T = 0.3 \end{cases} . \tag{3.14}$$

It is certainly remarkable, that when the p_T^{-4}-QCD processes are dominant, the predicted ratio of prompt photon to total π^+ production is as large as 250% at $\varepsilon = 0.3$. At present energies, however, the p_T^{-4}-QCD processes do not yet

seem to be dominant, at least for $p_T < 8$ GeV/c . The observed π^+-spectra, for example, go like p_T^{-8} at fixed x_T and θ_{cm} rather than p_T^{-4} as predicted by QCD. Consequently, we expect $\gamma_{QCD}/\pi^+_{expt}$ to be small and, indeed with

$$E\frac{d\sigma}{d^3p}(pp \to \pi^+ X)_{expt} \simeq 9\frac{\varepsilon^9}{p_T^8} \tag{3.15}$$

(in GeV units), we have

$$\frac{\gamma_{QCD}}{\pi^+_{expt}} \simeq [\alpha_\gamma F^\gamma_{BR}(\varepsilon) + \frac{\alpha}{\alpha_s} F^\gamma_{PR}(\varepsilon)]\frac{\alpha_s^2}{9}\frac{p_T^4}{\varepsilon} \simeq$$

$$\simeq 8 \times 10^{-5}\, p_T^4 \quad ; \qquad (\varepsilon \sim 1) \quad . \tag{3.16}$$

For $\sqrt{s} = 45$ GeV , $p_T = 3.7$ GeV/c , $\varepsilon = 0.84$, this gives $\gamma_{QCD}/\pi^+_{expt} \sim 1.4\%$, compared to the experimental value[9] $\sim 25\%$. In the next section we consider other sources of prompt photons, which will turn out to be dominant at such moderate p_T.

IV. p_T^{-6} AND p_T^{-8} - CIM CONTRIBUTIONS

Large momentum transfer processes involving bound states of fundamental fields can be analysed in terms of the minimum number of fields interacting in a hard scattering subprocess. This approach leads to a quite natural expansion of the complex interaction into a series of different types of subprocesses, each of them characterized by a large net momentum transfer. In reference 17, this hard scattering expansion is studied quantitatively; in a ϕ^3-theory, the leading processes give already 90% of the total cross section. The same rules applied to QCD lead to a series starting with the p_T^{-4}-processes of Section III, followed by processes of greater complexity such as $qg \to q'M$, $qM' \to q'M$ or $qB' \to q'B$ with M' , B' being low mass $q\bar{q}$ and qqq constituent states emitted by the colliding hadrons. Such processes, where the trigger hadron is formed before the high p_T scattering, can dominate over processes where the hadron is fragmented subsequent to the interaction, since the latter are suppressed by the fragmentation power in (2.7).[12] We will not go into a detailed discussion, which can be found in references 5, 11 and 17. However, we want to make at least some remarks.

The fall off in p_T of the contribution from a given subprocess is steeper the more "hot" gluons are exchanged. The higher order processes mentioned above have characteristic p_T^{-6}, p_T^{-8} and p_T^{-12} - CIM spectra, respectively, at fixed x_T and θ_{cm}. The absolute normalization of these contributions can be expressed in terms of the effective coupling constants α_s for quark to gluon, α_M for quark to meson and α_B for quark to baryon. A preliminary determination of α_s has been obtained from high p_T inclusive scattering [reference 11 and (3.1)]; α_M and α_B were determined from fixed angle elastic scattering and momentum sum rules[5] giving

$$\alpha_M \simeq 2\ \text{GeV}^2 \qquad \text{and} \qquad \alpha_B \simeq 10\ \text{GeV}^4 \quad . \tag{4.1}$$

For these values, the main source for pions at $p_T < 8$ GeV/c is the $qM \to q'\pi$ subprocess where M is constrained to contain the correct antiquark flavor of the observed pion.[18] The result

$$E\frac{d\sigma}{d^3p}(pp \to \pi^+) \simeq 1.1\,\alpha_M^2\frac{\varepsilon^9}{p_T^8} \tag{4.2}$$

is consistent with the experimental spectrum (3.15) taking into account other π^+ sources, especially resonance decay like $\rho^o \to \pi^+\pi^-$.[5]

Naturally, such higher order processes must also exist in the case of photon production. As at the p_T^{-4}-QCD level, we have prompt processes (Figure 5A) yielding p_T^{-6} terms and final bremsstrahlung processes (Figure 5B) giving rise to p_T^{-6} and p_T^{-8} contributions.

A. Prompt Processes:

(a) $qM \to q'\gamma$:

In the scaling limit, the cross section for this subprocess is given by[5]

$$\frac{d\sigma}{dt}(qM \to q'\gamma) = \frac{2\pi\alpha\alpha_M}{s^2}\frac{s^2+u^2}{t}\left(\frac{\lambda_{\bar{q}}}{u} - \frac{\lambda_{q'}}{s}\right)^2 \quad . \tag{4.3}$$

Then, according to (2.3) and Table I:

$$E\frac{d\sigma}{d^3p}(pp \to \gamma) = I\frac{\varepsilon^9}{p_T^6} \tag{4.4}$$

with[19]

$$I = 2\alpha\alpha_M \sum_{\substack{q\in p \\ \text{color}}} \sum_{M\in p} f_{q/p}\, N(q/p)\, f_{M/p}\, N(M/p) \quad (\lambda_{\bar{q}} + \tfrac{1}{2}\lambda_{q'})^2$$

$$\times 5 \times 2^6 \frac{\Gamma(5)\,\Gamma(7)}{\Gamma(10)}$$

$$\simeq 2\alpha\alpha_M \times 5 \times 2^6 \times \frac{1}{21} \times 1.2 \times 2.4 \times 0.1 \times$$

$$\times \left[0.3 \times \left\{ \left[-\frac{2}{3} + \frac{1}{2}\frac{2}{3} \right]^2 \times 3 + \left[-\frac{2}{3} + \frac{1}{2}\left(-\frac{1}{3} \right) \right]^2 \right\} + \right.$$

$$\left. + 0.2 \times \left\{ \left[\frac{1}{3} + \frac{1}{2}\frac{2}{3} \right]^2 \times 2 + \left[\frac{1}{3} + \frac{1}{2}\left(-\frac{1}{3} \right) \right]^2 \times 2 \right\} \right]$$

$$\simeq 4.4\alpha\alpha_M \ .$$

(b) $q\bar{q}' \to \gamma M$:

$$\frac{d\sigma}{dt}(q\bar{q}' \to \gamma M) = \frac{\pi\alpha\alpha_M}{s^2} \frac{t^2+u^2}{s} \left(\frac{\lambda_{\bar{q}}}{t} - \frac{\lambda_{q'}}{u} \right)^2 \tag{4.5}$$

and, consequently,

$$E\frac{d\sigma}{d^3p}(pp \to \gamma) = I \frac{\varepsilon^{11}}{p_T^6} \tag{4.6}$$

with

$$I \simeq \alpha\alpha_M \sum_{\substack{q\in p \\ \text{color}}} \sum_{\bar{q}'\in p} f_{q/p}\, N(q/p)\, f_{\bar{q}'/p}\, N(\bar{q}'/p)(\lambda_{\bar{q}} - \lambda_{q'})^2$$

$$\times 2^8 \frac{\Gamma(5)\,\Gamma(9)}{\Gamma(12)}$$

$$\simeq \alpha\alpha_M \times 2^8 \times \frac{4}{165} \times 1.2 \times 0.01$$

$$\times \left[0.3 \times \left\{ \left(-\frac{2}{3} - \frac{2}{3} \right)^2 + \left(-\frac{2}{3} + \frac{1}{3} \right)^2 \right\} \right.$$

$$\left. + 0.2 \times \left\{ \left(\frac{1}{3} - \frac{2}{3} \right)^2 + \left(\frac{1}{3} + \frac{1}{3} \right)^2 \right\} \right]$$

$$\simeq 0.05\, \alpha\alpha_M$$

ignoring strange antiquarks.

We see that the latter contribution is very much smaller than the yield from $qM \to q'\gamma$ and can be neglected.

B. Final Bremsstrahlung

(a) $qM \to q'g(q' \to \gamma)$:

Using the result for u and d jet production in $qM \to q'g$ given in reference 11:

$$E \frac{d\sigma}{d^3p}(pp \to u,d) = \frac{\varepsilon^9}{p_T^6} \alpha_s\, \alpha_M \times [0.06, 0.04] \qquad (4.7)$$

we obtain from (2.7):

$$E\frac{d\sigma}{d^3p}(pp \to \gamma) = \frac{\alpha_\gamma}{\pi}\ \frac{1}{10}\ \left(\frac{4}{9}\times 0.06 + \frac{1}{9}\times 0.04\right) \times \alpha_s\,\alpha_M\,\frac{\varepsilon^{10}}{p_T^6}$$

$$= 1\times 10^{-3}\,\alpha_\gamma\,\alpha_M\,\alpha_s\,\frac{\varepsilon^{10}}{p_T^6} \quad . \tag{4.8}$$

(b) $qM' \to q'M(q' \to \gamma)$:

Since any meson M can contribute to the production of the q'-quark jet, we have to multiply the corresponding π^+-cross section by the number of participating mesons:

$$E\frac{d\sigma}{d^3p}(pp \to q'\text{-jet}) = N(M)\ E\frac{d\sigma}{d^3p}(pp \to \pi^+) \quad . \tag{4.9}$$

Estimating N(M) as $9+3\times 9 = 36$ for spin 0 and spin 1 meson nonets, one obtains with (4.2), (2.7) and $\langle\lambda_u^2 + \lambda_d^2\rangle = \frac{5}{18}$:[20]

$$E\frac{d\sigma}{d^3p}(pp \to \gamma) \simeq \frac{\alpha_\gamma}{\pi}\ \frac{1}{10}\ \frac{5}{18}\ 36\times 1.1\,\alpha_M^2\,\frac{\varepsilon^{10}}{p_T^8}$$

$$\simeq 0.4\,\alpha_\gamma\,\alpha_M^2\,\frac{\varepsilon^{10}}{p_T^8} \quad . \tag{4.10}$$

Both contribution (a) and (b) are small compared to (4.4):

$$\frac{\gamma(qM \to q'g\gamma)}{\gamma(qM \to q'\gamma)} \sim 1.4\times 10^{-4}\varepsilon \quad , \quad \frac{\gamma(qM' \to q'M\gamma)}{\gamma(qM \to q'\gamma)} \sim 0.7\,\frac{\varepsilon}{p_T^2} \tag{4.11}$$

and may be neglected. The same is true for other sources like $qg \to q'M\gamma$, $Mg \to q'\bar{q}\gamma$ or $qB' \to q'B\gamma$.

We clearly see that the prompt process $qM \to q'\gamma$ is by far the dominant CIM source for high p_T photons yielding[5]

$$E\frac{d\sigma}{d^3p}(pp \to \gamma X) \simeq 4.4\alpha\alpha_M \frac{\varepsilon^9}{p_T^6} \tag{4.12}$$

and (in GeV units)

$$\frac{\gamma_{CIM}}{\pi^+_{expt}} \simeq 0.48\alpha\alpha_M p_T^2 \simeq 0.007\, p_T^2 \tag{4.13}$$

if we use the form (3.15) for π^+_{expt} and $\alpha_M = 2$. For $p_T = 3.7$ GeV/c, this gives $\gamma_{CIM}/\pi^+_{expt} \sim 10\%$, which is much larger than corresponding value of $\sim 1.4\%$ for the p_T^{-4}-QCD sources but less than the ISR result[9] of $\sim 25\%$. Together, the QCD and CIM contributions should describe the γ production and the $\frac{\gamma}{\pi}$ ratios from moderate up to very high p_T. This complete description is the main topic of our concluding discussion.

V. DISCUSSION AND CONCLUSION

Let us summarize our results obtained in Section III and IV. We have shown that the two leading terms in the hard scattering expansion[17] of the inclusive production of prompt photons at high p_T and $\theta_{cm} = 90°$ in pp collisions, $pp \to \gamma X$, are given by the p_T^{-4}-term from prompt processes and final bremsstrahlung (3.10):

$$[\alpha_s^2 \alpha_\gamma F_{BR}^{\gamma}(\varepsilon) + \alpha_s \alpha F_{PR}^{\gamma}(\varepsilon)] \frac{\varepsilon^8}{p_T^4} \tag{5.1}$$

and the p_T^{-6}-term from the prompt CIM process (4.4):

$$4.4 \alpha_M \alpha \frac{\varepsilon^9}{p_T^6} \quad . \tag{5.2}$$

Other p_T^{-6} terms as well as p_T^{-8} and higher power terms (4.6, 8, 10) only contribute at the few % level and become completely negligible as p_T increases. For π^+-production, the asymptotic series is dominated by the QCD-p_T^{-4}-term [Table III and (3.13)]:

$$\alpha_s^2 F_{QCD}^{\pi}(\varepsilon) \frac{\varepsilon^9}{p_T^4} \tag{5.3}$$

and the CIM p_T^{-8} term:

$$2.25 \alpha_M^2 \frac{\varepsilon^9}{p_T^8} \quad . \tag{5.4}$$

The latter term follows from (4.2) after multiplication by the appropriate $\pi^+_{expt}/\pi^+_{prompt}$ ratio (~2) to account for the experimental spectrum $E \frac{d\sigma}{d^3p}(pp \to \pi^+ X)_{expt} = 9 \frac{\varepsilon^9}{p_T^8}$ at moderate p_T.[21] There are possibly some

corrections due to scaling violations. However, we do not expect them to change our results in a crucial way.

Finally, the prompt γ to total π^+ ratio R_{γ/π^+} at $\theta_{CM} = 90°$ is given by:

$$R_{\gamma/\pi^+} = \frac{[\alpha_s^2 \alpha_\gamma F_{BR}^\gamma(\varepsilon) + \alpha_s \alpha F_{PR}^\gamma(\varepsilon)] p_T^4 + 4.4\, \alpha\alpha_M \varepsilon p_T^2}{[2.25\, \alpha_M^2 + \alpha_s^2 F_{QCD}^\pi(\varepsilon) p_T^4] \varepsilon} \quad . \tag{5.5}$$

It is plotted in Figure 6 for FNAL, ISR and future "asymptotic" energies as a function of p_T taking for the coupling constants the values (3.1) and (4.1). Figures 7 and 8 show the scaling behavior. The main features are:

(1) strong energy dependence at fixed p_T for high p_T;

(2) increasing energy independence at fixed ε as $\sqrt{s}$ increases due to the dominance of p_T^{-4}-QCD processes;

(3) if QCD dominates $R_{\gamma/\pi} \sim \frac{1}{\varepsilon} \to \infty$ as $\varepsilon \to 0$;

(4) at low to moderate p_T CIM dominates and $R_{\gamma/\pi} \sim p_T^2$ independent of ε .

It is also interesting to see that at very, very high energies a clear separation between the CIM- and QCD-dominated p_T regions develops, indicated by a dip in R_{γ/π^+} (Figure 6).

To investigate the interaction between QCD and CIM further, we calculate the ratio of the p_T^{-4} to the p_T^{-6} contributions to $pp \to \gamma X$. Taking the same values for the coupling constants as above, we find

$$\frac{\gamma_{QCD}(p_T^{-4})}{\gamma_{CIM}(p_T^{-6})} \simeq \begin{cases} 1.2 \times 10^{-2}\, p_T^2 & ; \quad \varepsilon = 0{,}7 \\ 1.5 \times 10^{-2}\, p_T^2 & ; \quad \varepsilon = 0{,}5 \end{cases} \tag{5.6}$$

This implies a cross over from CIM to QCD dominance at $p_T^\gamma \simeq 8.3$ GeV/c at $\sqrt{s} \simeq 33$ GeV and $p_T^\gamma \simeq 9.2$ GeV/c at $\sqrt{s} \simeq 61$ GeV. In contrast, the cross over

between QCD(p_T^{-4}) and CIM(p_T^{-8}) contributions to π production occurs at $p_T^{\pi} \simeq 10.7$ GeV/c and $p_T^{\pi} \simeq 8.2$ GeV/c at the same energies, respectively [see reference 11 and equations (5.3) and (5.4)]. We can thus distinguish three regions:

(I) The CIM contributions ($Mq \to \gamma q$, $Mq \to Mq$) dominate both γ and π production. The photons are produced directly in the hard scattering subprocess. In this region, where p_T is typically below 8 GeV/c at ISR energies, $E\, d\sigma/d^3p \sim p_T^{-8}$ for pions and $\gamma/\pi \sim 0.7\%\ p_T^2$ at fixed θ_{cm} [see (4.13) and Figure 6]. In Figure 8, this region is characterized by a linear rise of R with s at fixed ε .

(II) The QCD (p_T^{-4}) contributions dominate both γ and π production. In this region, a typical p_T of which is beyond $p_T \simeq 10$ GeV/c at ISR energies, the γ/π ratio is independent of p_T at fixed ε (Figure 8) and grows like $\sim \frac{1}{\varepsilon}$ [see (3.11) and Figure 7]. The main photon source is the prompt subprocess $gq \to \gamma q$ producing a pure electromagnetic jet. Experimental implications of this fact have been discussed in the Introduction. The QCD bremsstrahlung ($qq \to qq\gamma$, etc.) contributes at maximum 20% of the prompt process and considerably less (~5%) at smaller ε . The rise of $\frac{\gamma}{\pi}$ as $\varepsilon \to 0$ indicates that at the edge of phase space, the pointlike electromagnetic production can become stronger than the production of hadrons.

(III) Below $\sqrt{s} \simeq 48$ GeV , there is an intermediate region where the QCD(p_T^{-4}) contributions already dominate the photon spectrum, whereas the π production is still dominated by the CIM(p_T^{-8}) contribution. Above $\sqrt{s} \simeq 48$ GeV just the opposite occurs; the intermediate region is characterized by QCD dominance

of the π spectrum and CIM dominance of the photon spectrum. This switch-over, illustrated in Figure 9, is sensitive to the particular power ($g_{g/p} = 4$) of the proton's gluon distribution.

We should stress that the balance sheet of subprocesses described here for real photons depends strongly on M_γ^2 in the case of virtual photons. It is also of interest to consider γ-production for other beams such as $\pi^\pm$ or $\bar{p}$ where the $q\bar{q} \to \gamma g$ p_T^{-4}-subprocess can play a more important role.[22]

We have thus achieved a rather complete description of the production of high p_T photons from the basic assumption of a pointlike photon-quark coupling in QCD and CIM subprocesses. Our numerical results for the various cross sections should be reliable up to a factor of 2-3 due to the inherent uncertainty in the absolute normalizations and in the choice of the structure and fragmentation parameters. This uncertainty is obviously somewhat less for the $\frac{\gamma}{\pi}$ ratios. So far, there is only one measurement[9] of $\frac{\gamma}{\pi}$ at relatively small p_T (~3 GeV), where we predict CIM to be dominant. Our result is consistent with these data, as far as the order of magnitude is concerned as well as the rise with p_T. A more complete test of our predictions does not seem to represent an unsolvable experimental problem. We would like to encourage such experiments, especially a combination of a photon trigger and a hadron veto on the trigger side suggested in the Introduction.

APPENDIX A: PHOTON FRAGMENTATION FUNCTION

In our calculations of the photon yield from final bremsstrahlung processes, we used an effective fragmentation function of a quark into a photon of the form

$$w\, D_{\gamma/q}(w) = \frac{\lambda_q^2}{\pi}\,\alpha_\gamma \tag{A.1}$$

with $\alpha_\gamma \simeq \alpha\, \ell n \frac{\sqrt{s}}{m_q}$ [see (2.5) and (2.6)]. Here we want to show that (A.1) follows from a pure first order QED calculation with a pointlike q-γ coupling. To simplify the discussion, we may assume that only one charged constituent participates in the process (e.g. $gq \to gq\gamma$ or Figure 2). A characteristic and, in the following, very essential feature of any final bremsstrahlung process is the large momentum transfer in the underlying nonradiative process (e.g. $gq \to gq$).

Although we are interested in the production of hard photons, it is sufficient for our purpose to study the soft or classical radiation which shows the same main features, at least in the kinematical region we are considering. In this approximation, the differential cross section for producing a photon with momentum k is given by[23]

$$\frac{d\sigma}{d^3k/k_o dt} \simeq \frac{dN_\gamma}{d^3k/k_o}\,\frac{d\sigma_o}{dt} \tag{A.2}$$

where $\frac{d\sigma_o}{dt}$ is the cross section of the underlying nonradiative process (e.g. $gq \to gq$) and

$$\frac{dN_\gamma}{d^3k/k_o} = \frac{\alpha\lambda_q^2}{4\pi^2}\sum_{pol}\left|\frac{\varepsilon\cdot p'}{k\cdot p'} - \frac{\varepsilon\cdot p}{k\cdot p}\right|^2 . \tag{A.3}$$

$p(p')$ is the initial (final) quark momentum and ε is the photon polarization vector. Integration of (A.3) over the solid angle of the photon leads to the energy spectrum

$$\frac{dN}{dk_o/k_o} \simeq \frac{2\alpha\lambda_q^2}{\pi} \left(\ell n \frac{|t|}{m_q^2} - 1\right) \tag{A.4}$$

if $|t| >> 4m_q^2$. In the Lorentz gauge, the dominant ℓn-term comes solely from the interference term in (A.3). In the Coulomb gauge, however, the situation is quite different. Each of the two square terms of (A.3) describes the intensity of the radiation at a given frequency k_o concentrated in narrow cones around the direction of radiating particle. These contributions are independent of t and for $s >> 4m_q^2$ given by $\frac{\alpha\lambda_q^2}{\pi} \left(\ell n \frac{s}{m_q^2} - 2\right)$ per particle. The interference term, on the other hand, knows of the momentum transfer to the quark current. It gives $\frac{2\alpha\lambda_q^2}{\pi} \left(\ell n \frac{|t|}{s} + 1\right)$ and all three terms together add up to (A.4). This shows clearly that in the Coulomb gauge and at large t the photon yield at large angle in the center of mass system is to a large extent dominated by the radiation from the scattered quark, in other words by final bremsstrahlung. So

$$\frac{d\sigma}{dk_o dt} \simeq \frac{dN_\gamma^{FBR}}{dk_o} \frac{d\sigma_o}{dt} \tag{A.5}$$

with $\frac{dN_\gamma^{FBR}}{dk_o/k_o} \simeq \frac{\alpha\lambda_q^2}{\pi} \ell n \frac{s}{m_q^2}$. A more rigorous calculation,[24] including spin, valid for all photon energies with the exception of the end of the spectrum, gives for the leading logarithmic term

$$\frac{dN_\gamma^{FBR}}{dk_o/k_o} \simeq \frac{\alpha\lambda_q^2}{\pi} \ell n \left[\frac{s}{m_q^2} \left(1 - \frac{2k_o}{\sqrt{s}} \right) \right] \frac{1 + \left(1 - \frac{2k_o}{\sqrt{s}} \right)^2}{2} \quad . \tag{A.6}$$

In terms of the light cone fraction w and the transverse momentum k_T of the photon relative to the scattered intermediate quark, the formulas are slightly more complicated, for example:[25]

$$w \frac{dN_\gamma^{FBR}}{dw\, dk_T^2} \simeq \frac{\alpha\lambda_q^2}{\pi} \frac{k_T^2}{\left(1 + \frac{k_T^2}{w^2 s} \right)^2 \left(w^2 m_q^2 + k_T^2 \right)^2} \quad . \tag{A.7}$$

This result corresponds to the $(\varepsilon \cdot p')^2$ term in Eq. (A.3) where $s' \equiv (p_0' + p_3')^2$.

The leading term of $w \frac{dN_\gamma^{FBR}}{dw}$, however, is the same as in (A.5) or (A.6). One only has to replace $\frac{2k_o}{\sqrt{s}}$ by w :

$$w \frac{dN_\gamma^{FBR}}{dw} = \frac{\alpha\lambda_q^2}{\pi} \ell n \left(\frac{s(1-w)}{m_q^2} \right) \frac{1 + (1-w)^2}{2} \quad . \tag{A.8}$$

$$\equiv w\, D_{\gamma/q}(w) \quad .$$

Finally, the contribution from the $(1-w)^2$ term becomes negligible, after smearing out by the proton structure functions (see footnote 12). So, we obtain an effective fragmentation function of the form (A.1).

APPENDIX B: PRODUCTION OF HIGH p_T PHOTONS IN A ϕ^3-PARTON MODEL

As an instructive example how the elementary nature of the photon reveals itself at large transverse momentum, we will consider a parton model which leads asymptotically to a p_T^{-8}-spectrum for pions. Such a model was proposed some time ago by R. D. Field and R. P. Feynman.[1] Although this model can now be ruled out on phenomenological grounds,[26] we shall use it here to show that the growth of $\frac{\gamma}{\pi} \sim \alpha p_T^2$ at fixed ε and θ_{cm} is a general attribute of any model which yields p_T^{-6} or faster behavior for hadron production, but has point-like couplings of photons to the quark current.

In the Field-Feynman Model the cross section for $qq \to qq$ is determined phenomenologically from data as

$$\frac{d\sigma}{dt}(qq \to qq) = \frac{C}{s(-t)^3} \tag{B.1}$$

where $C = 2.3\ \text{b GeV}^6 = 5.9 \times 10^3\ \text{GeV}^4$. Equation (2.3) and Table I predict, then, for u and d quark production:

$$E\frac{d\sigma}{d^3p}(pp \to u,d) = \frac{\varepsilon^7}{p_T^8}[I_u, I_d] \tag{B.2}$$

with $[I_u, I_d] = \frac{C}{\pi} 2^4 \frac{\Gamma(5)\,\Gamma(5)}{\Gamma(8)} (1.2)^2 [0.3(0.3 + 0.2),\ 0.2(0.3 + 0.2)]$

$$\simeq [754, 503] \quad .$$

This gives, according to (2.9), the following $\frac{\gamma}{\pi^+}$ ratio for γ's produced via final bremsstrahlung:

$$\frac{\gamma}{\pi^+} \simeq \frac{\frac{\alpha_\gamma}{\pi}}{d_{\pi^+/u}} \frac{\left(\frac{4}{9} I_u + \frac{1}{9} I_d\right)}{I_u} \frac{9}{\left(1 - \frac{\varepsilon}{8}\right)^2 \varepsilon} \quad . \tag{B.3}$$

Then, taking $d_{\pi^+/u} \sim 0.5$ and $\alpha_\gamma \simeq 4\alpha$:

$$\frac{\gamma}{\pi^+} \simeq \frac{0.10}{\varepsilon} \quad . \tag{B.4}$$

Final state bremsstrahlung alone, however, is not gauge invariant. In section II we have sketched how gauge invariance is restored by the prompt processes. Thus, they should also be present in the Field-Feynman Model. The problem is that there is no straightforward way to calculate them since the basic cross section (B.1) is a phenomenological ansatz rather than the result of an underlying field theory. Therefore, we consider a simple field theoretic model for (B.1). Since $t = -\frac{s}{2}$ at $\theta_{cm} = 90°$ we can write

$$\frac{d\sigma}{dt}(qq \to qq) \simeq \frac{2C}{s^2 t^2} \quad , \tag{B.5}$$

which can be interpreted as the cross section for qq scattering in a ϕ^3-theory of spin 0 quarks and quarklike gluons "g" (Figure 10):

$$\frac{d\sigma}{dt}(qq \to qq) = \frac{g^4}{16\pi s^2}\frac{1}{t^2} \quad . \tag{B.6}$$

Comparison of (B.5) and (B.6) fixes the coupling constant $\alpha_F = \frac{g^2}{4\pi} = 61\ \text{GeV}^2$. One can check that this form together with the parameters given in Tables I and II gives the correctly normalized cross section $E\, d\sigma/d^3p\ (pp \to \pi^+ X)$ $\sim 9\ \varepsilon^9/p_T^8$ at $\theta_{cm} = 90°$ for $p_T < 8$ GeV within a factor of 2.

We now calculate the photon spectrum arising from the prompt subprocess $q"g" \to q\gamma$ (Figure 11), the analogue of $qg \to q\gamma$ in QCD:

$$\frac{d\sigma}{dt}(q"g" \to q\gamma) = 4\pi\, \alpha_F \alpha\, \lambda_q^2 \frac{t}{s^3 u} \quad . \tag{B.7}$$

For this purpose, we need the distribution function $G_{"g"/p}$ of the "gluons" inside the proton. A reasonable choice is the form suggested by dimensional analysis:

$$G_{"g"/p} \simeq 6 f_{"g"/p} \frac{(1-x)^5}{x} \tag{B.8}$$

where we will use the usual gluon normalization $f_{"g"/p} \sim 0.5$. The γ spectrum follows, then, from (2.3)

$$E \frac{d\sigma}{d^3p} (pp \to \gamma) \simeq 4\alpha \alpha_F 1.2 \left(\frac{4}{9} 0.3 + \frac{1}{9} 0.2 \right) 0.5 \times 2^5 \times \frac{\Gamma(5)\,\Gamma(7)}{\Gamma(10)} \frac{\varepsilon^9}{p_T^6} \tag{B.9}$$

$$\simeq 0.57\, \alpha\alpha_F \frac{\varepsilon^9}{p_T^6} \quad .$$

Thus, our ϕ^3-model leads to a $\frac{\gamma}{\pi}$ ratio which rises with p_T^2:

$$\frac{\gamma}{\pi^+} \sim 0.03\, p_T^2 \quad . \tag{B.10}$$

The effective q-q interaction in the Field-Feynman Model could certainly be more complicated than assumed in (B.6). Yet dimensional analysis would still give $\frac{\gamma}{\pi} \sim \alpha\, p_T^2$ for promptly produced photons.[27] This result simply reflects the pointlike coupling of the photon to the quark current and can be expected to hold for all models which yield hadron spectra $\sim p_T^{-2N}$ with $N \geq 3$.

ACKNOWLEDGEMENTS

One of the authors (R.R.) is especially grateful to N. Byers for her continuous support and interest in his work. He also wishes to thank colleagues at the Department of Physics at UCLA for their kind hospitality and the Max-Planck-Institute for its generous financial support. The calculations of the CIM terms were done in collaboration with R. Blankenbecler. We also wish to thank R. Blankenbecler, W. Caswell, R. Horgan, and G. Farrar for helpful conversations.

REFERENCES

1. Among the large amount of literature on High p_T Physics see, for example, D. Sivers, S. J. Brodsky and R. Blankenbecler, Phys. Rep. 23C, 1 (1976) and references therein, and R. D. Field and R. P. Feynman, Phys. Rev. D15, 2590 (1977).

2. J. D. Bjorken and E. Paschos, Phys. Rev. 185, 1975 (1969). The production of real photons at large transverse momentum in hadron-hadron collisions has been considered by G. R. Farrar and S. Frautschi, Phys. Rev. Lett. 36, 1017 (1976); G. R. Farrar, Phys. Lett. 67B, 337 (1977); F. Halzen and D. M. Scott, Phys. Rev. Lett. 40, 1117 (1978). Our results differ quantitatively from those of these authors. A lower bound for the production of hard photons plus a recoiling gluon jet has been given by S. J. Brodsky, W. Caswell, and R. R. Horgan (to be published), reported by S. Brodsky in "Color Symmetry and Quark Confinement," Proc. of the XII. Recontre de Moriond, 1977.

3. W. Ochs and L. Stodolsky, Phys. Letters 69B, 225 (1977).

4. $D_{\gamma/q}$ is discussed in detail in Appendix A.

5. R. Blankenbecler, S. J. Brodsky and J. F. Gunion, SLAC preprint 2057 (1977).

6. R. Anderson et al., Phys. Rev. Letters 30, 627 (1973).

7. R. Marshall, Proceedings of the 1977 Int. Symp. on Lepton and Photon Interactions at High Energies, Hamburg;
M. A. Shupe et al., papers 159 and 168 submitted to this symposium.
Note that here we are, for sure, dealing with prompt photons.

8. A. M. Eisner et al., Phys. Rev. Letters 33, 865 (1974);
D. O. Caldwell et al., Phys. Rev. Letters 33, 868 (1974).

9. P. Darriulat, Proceedings of the XVIII Int. Conf. on High Energy Physics, Tbilisi (1977), Nucl. Phys. B110, 365 (1976).

10. The bremsstrahlung process $gq \to gq(q \to \gamma)$ contributes a very small percentage to the total γ-cross section at high p_T and is easily eliminated by the veto trigger.

11. J. F. Gunion, Talk presented at the SLAC Meeting on Large Transverse Momentum Phenomena, Jan. 27, 1978 UC Davis preprint, and references therein; Papers by R. Blankenbecler, S. J. Brodsky, J. F. Gunion and D. Jones in preparation.

12. In QED $wD_{\gamma/q} \sim 1 + (1-w)^2$. The second term, however, leads to a contribution suppressed by a factor $\frac{2\epsilon^2}{(F+2)(F+3)}$ $\left[= \frac{\epsilon^2}{45} \right.$ for a typical value of $F=7$ in (2.3)] relative to the first term and can be neglected. The effect of trigger bias is discussed in S. Ellis, M. Jacob and P. Landshoff, Nucl. Phys. B108, 93 (1976).

13. In reference 2, Farrar obtains $\frac{\gamma}{\pi^o} \sim$ 2-3% because of the assumption that the penalty for fragmentation is essentially the same for π and γ .

14. We only consider bremsstrahlung from the produced quark pair.

15. This value for α_s gives a result for $E\frac{d\sigma}{d^3p}(pp \to \pi^o)$ which is consistent with the preliminary ISR data from CCOR and R702 at $\sqrt{s} = 62$ GeV and $p_T \sim 7$ to 12 GeV/c (see reference 11).

16. The fragmentation of a gluon jet into a π^+ is not included.

17. W. Caswell, R. Horgan, and S. J. Brodsky, SLAC PUB 2106 (1978).

18. The p_T^{-6} contributions from $qg \to q'\pi$ are very small due to cancellations among the various terms appearing for gauge invariance (reference 11).

19. Note that if $\bar{q} = \bar{d}$ and $q = d$, q' is three times a u and once a d, and if $\bar{q} = \bar{d}$ and $q = d$, one has twice $q' = u$ and twice $q' = d$.

20. There is also radiation from the meson jet enhancing this result by roughly a factor 2 if we take $\langle\lambda_M^2\rangle \sim \frac{4}{9}$ for a nonet of mesons.

21. Arguments supporting $\pi^+_{prompt}/\pi^+_{total} \sim \frac{1}{2}$ are given in reference 5.

22. See also W. Caswell, R. Horgan and S. Brodsky, reference 2.

23. J. D. Bjorken and S. D. Drell, "Relativistic Quantum Mechanics," New York, McGraw-Hill, Inc., 1964.

24. N. Byers, R. Rückl and A. Yano, to be published.

25. See the work of S. Brodsky and J. F. Gunion as summarized in S. Brodsky, Proceedings of the XII. Rencontre de Moriond, 1977 (reference 2).

26. R. D. Field, Talk presented at the SLAC meeting on Large Transverse Momentum Phenomena, Jan. 27, 1978.

27. From the ϕ^3-simulation of the "old" Field-Feynman model (reference 1), we estimate for $\sqrt{s} = 45$ GeV , $p_T = 3.7$ GeV/c and $\theta_{cm} = 90°$: $\gamma/\pi^+ \approx 0.03\ p_T^2 + \frac{0.11}{\varepsilon} \sim 50\%$, dramatically rising forever as p_T increases.

FIGURE CAPTIONS

1. A schematic of the quark fragmentation functions
   - into a pion: $x D_{\gamma/q} \sim (1-x)^n$; $n = 1(a)$ or $2(b)$
   - into a photon: $x D_{\gamma/q} \sim 1 + (1-x)^2$ (see Appendix A).

2. Contributions to the gauge invariant amplitude for $qq \to qq\gamma$, neglecting radiation from the bottom quark line: (a) from "final" bremsstrahlung, (b) from "initial" bremsstrahlung.

3. Dominant configurations leading to high p_T photons in $qq \to qq\gamma$:
   (a) final bremsstrahlung with large momentum transfer in $qq \to qq$,
   (b) initial and final bremsstrahlung with large momentum transfer in $qg \to q\gamma$.

4. Feynman diagrams for the p_T^{-4}-QCD subprocesses yielding high p_T photons:
   A. final bremsstrahlung processes,
   B. prompt processes.

5. CIM processes yielding high p_T photons:
   A. prompt processes,
   B. final bremsstrahlung processes.

6. p_T dependence of $\frac{\gamma}{\pi^+}$ at $\theta_{cm} = 90°$ and $\sqrt{s} = 19.4$, 45, 62 and 800 GeV.

7. ε dependence of $\frac{\gamma}{\pi^+}$ at $\theta_{cm} = 90°$ and $\sqrt{s} = 19.4$, 45, 62 and 800 GeV.

8. Energy dependence of $\frac{\gamma}{\pi^+}$ at fixed $\varepsilon = 0.7$, 0.5 and 0.3.

9. Cross over from CIM to QCD in π and γ production.

10. qq scattering diagram in a ϕ^3 model.

11. Feynman diagrams for the prompt subprocess $q''g^n \to q\gamma$ yielding high p_T photons in a ϕ^3 model.

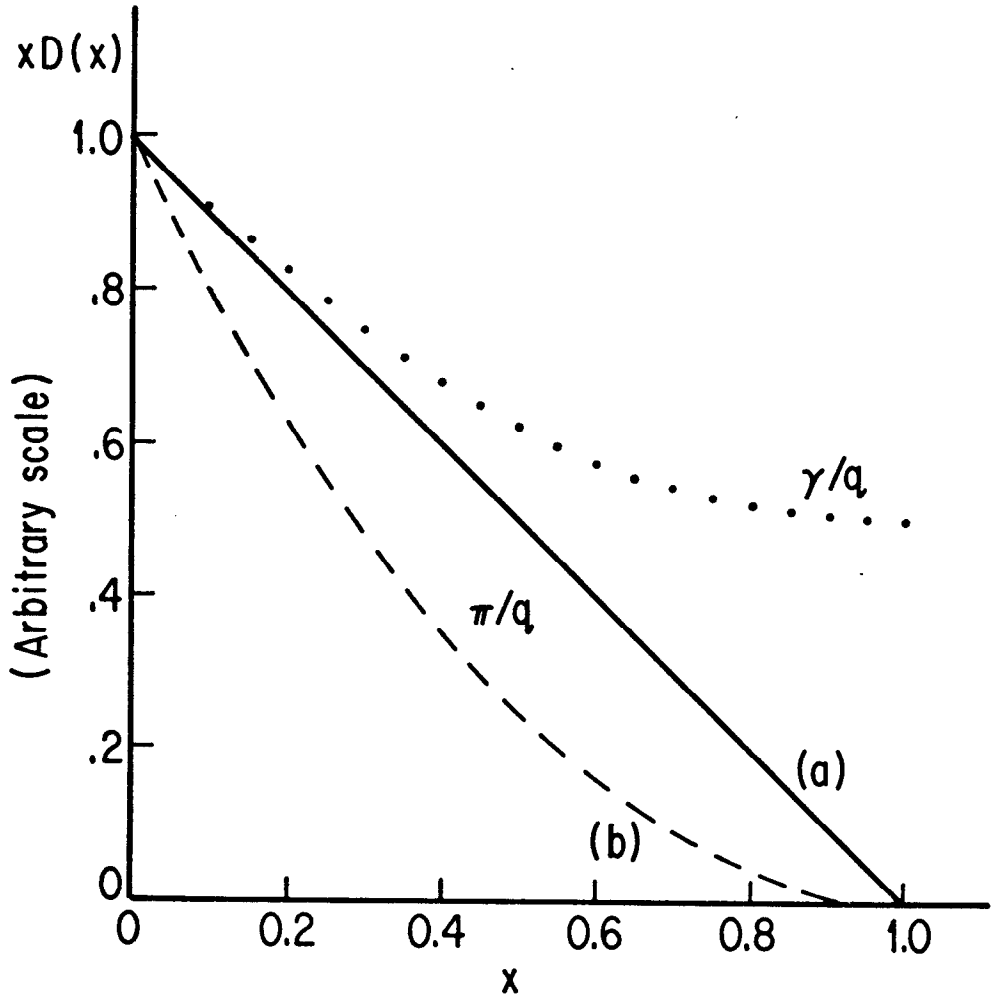

Fig. 1

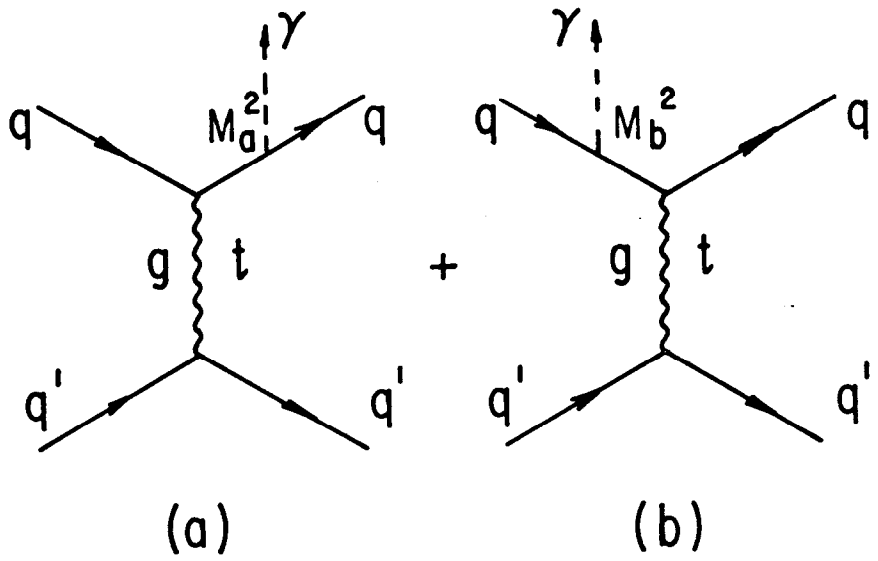

Fig. 2

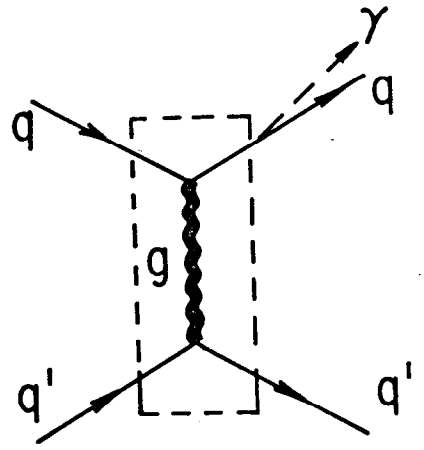

(a)

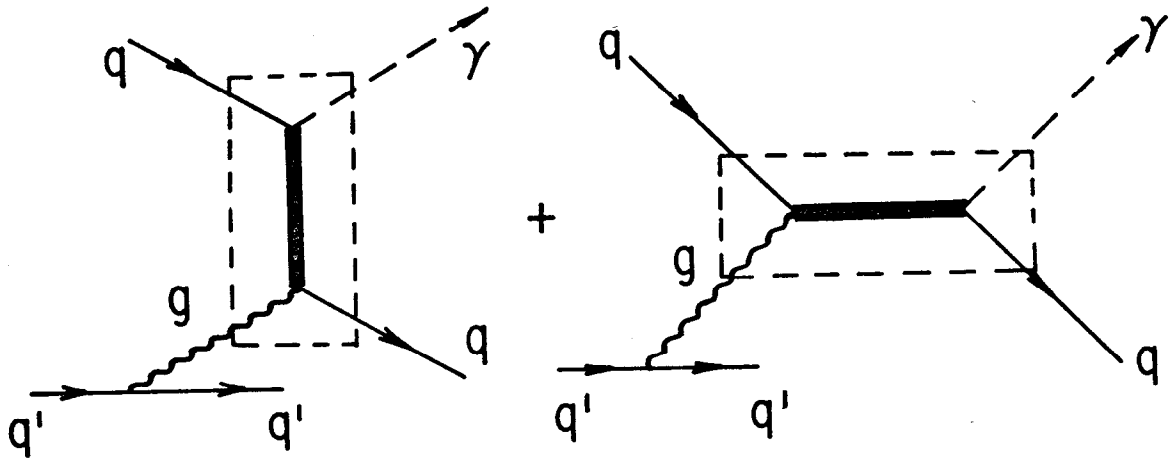

(b)

Fig. 3

(a) $qq \to qq(q \to \gamma)$

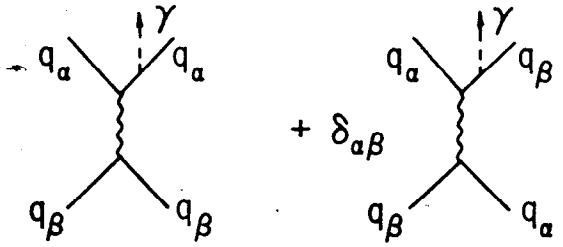

(b) $gq \to gq(q \to \gamma)$

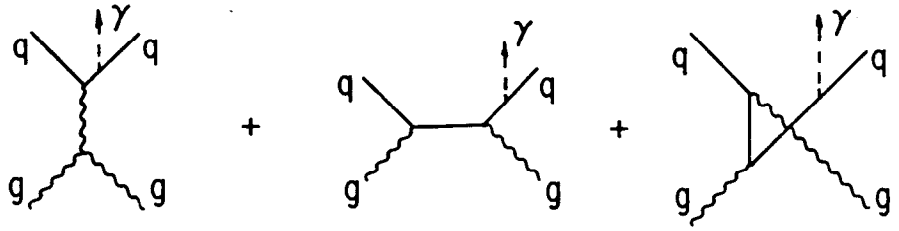

(c) $gg \to q\bar{q}\ (q, \bar{q} \to \gamma)$

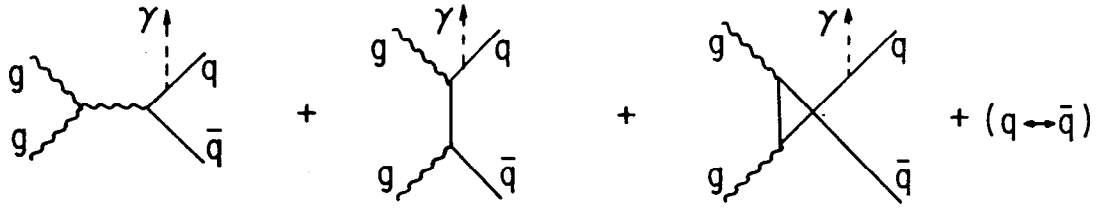

(d) $q\bar{q} \to q\bar{q}\ (q, \bar{q} \to \gamma)$

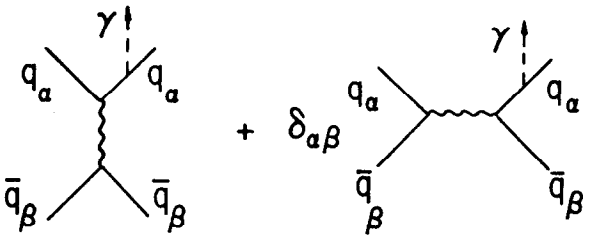

(e) $g\bar{q} \to g\bar{q}\ (\bar{q} \to \gamma)$ see (b)

Fig. 4a

(a) $gq \to \gamma q$

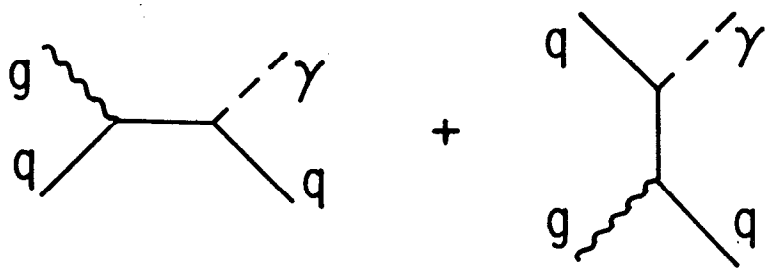

(b) $q\bar{q} \to g\gamma$

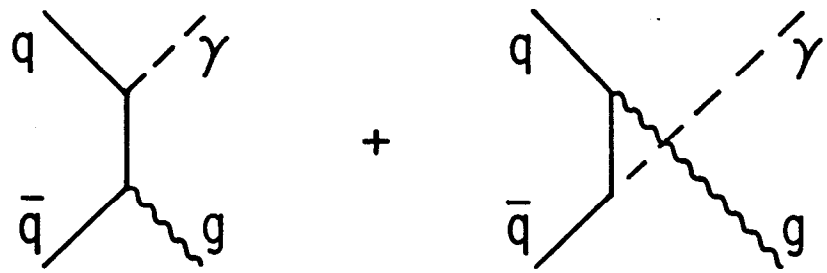

(c) $g\bar{q} \to \gamma\bar{q}$: see (a)

Fig. 4b

(a) $qM \to q'\gamma$

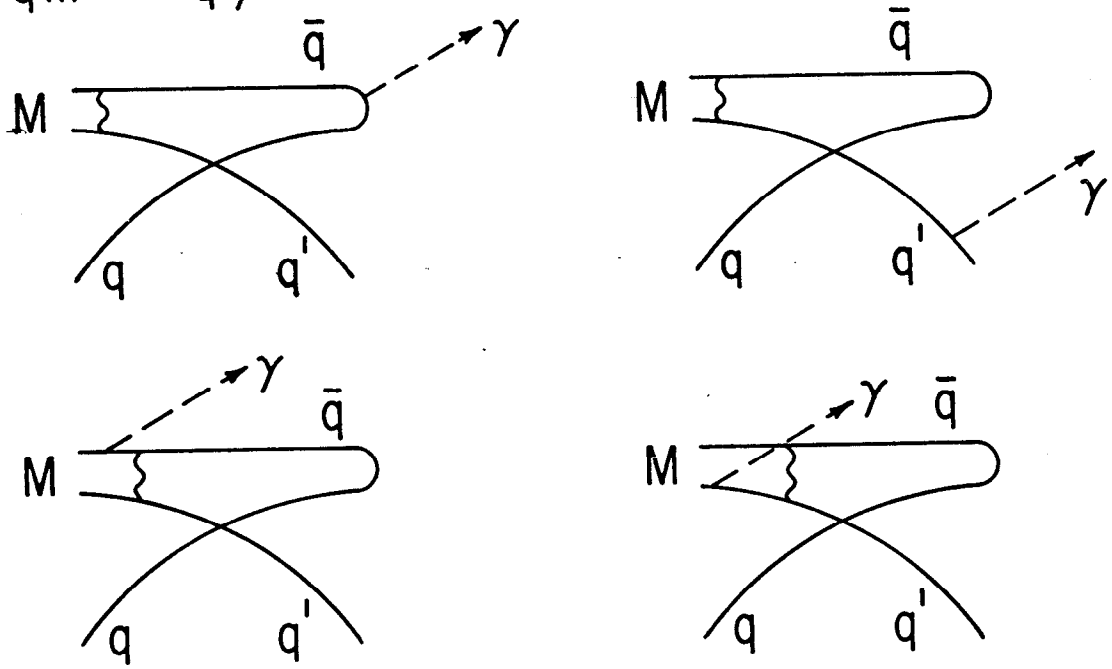

(b) $q\bar{q}' \to M\gamma$

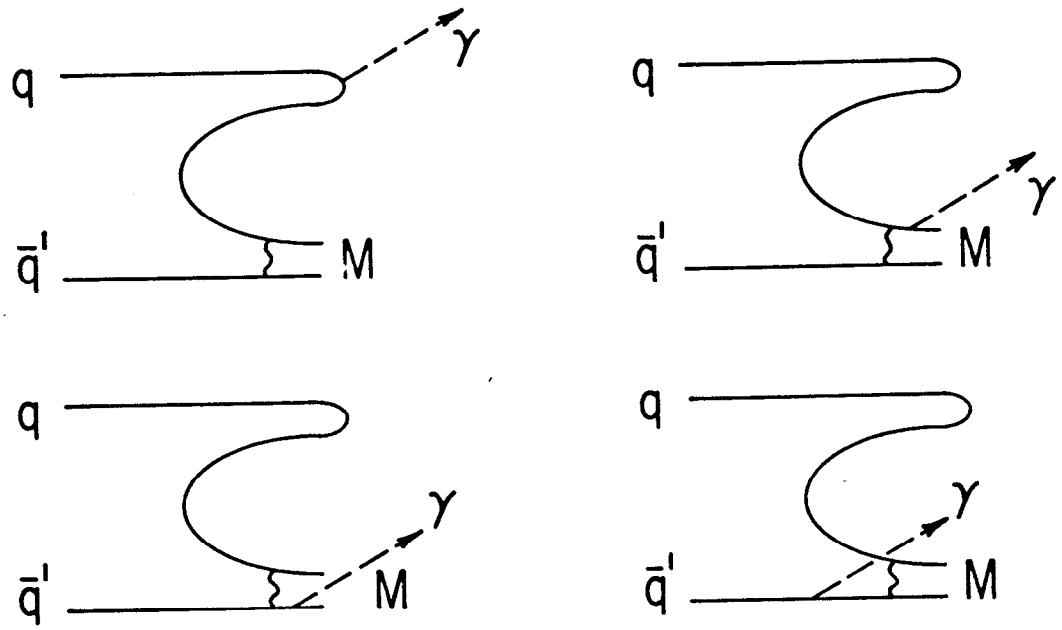

Fig. 5a

(a) $qM \rightarrow q'g\ (q' \rightarrow \gamma)$

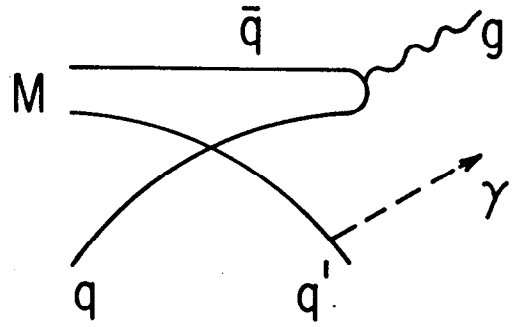

(b) $qM' \rightarrow q'M\ (q' \rightarrow \gamma)$

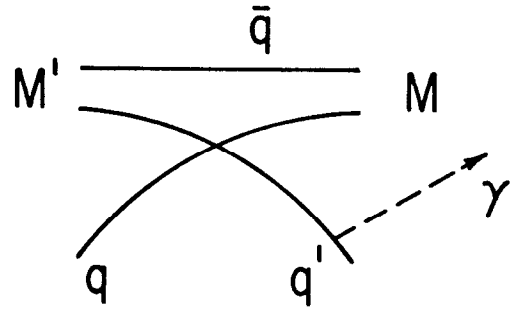

Fig. 5b

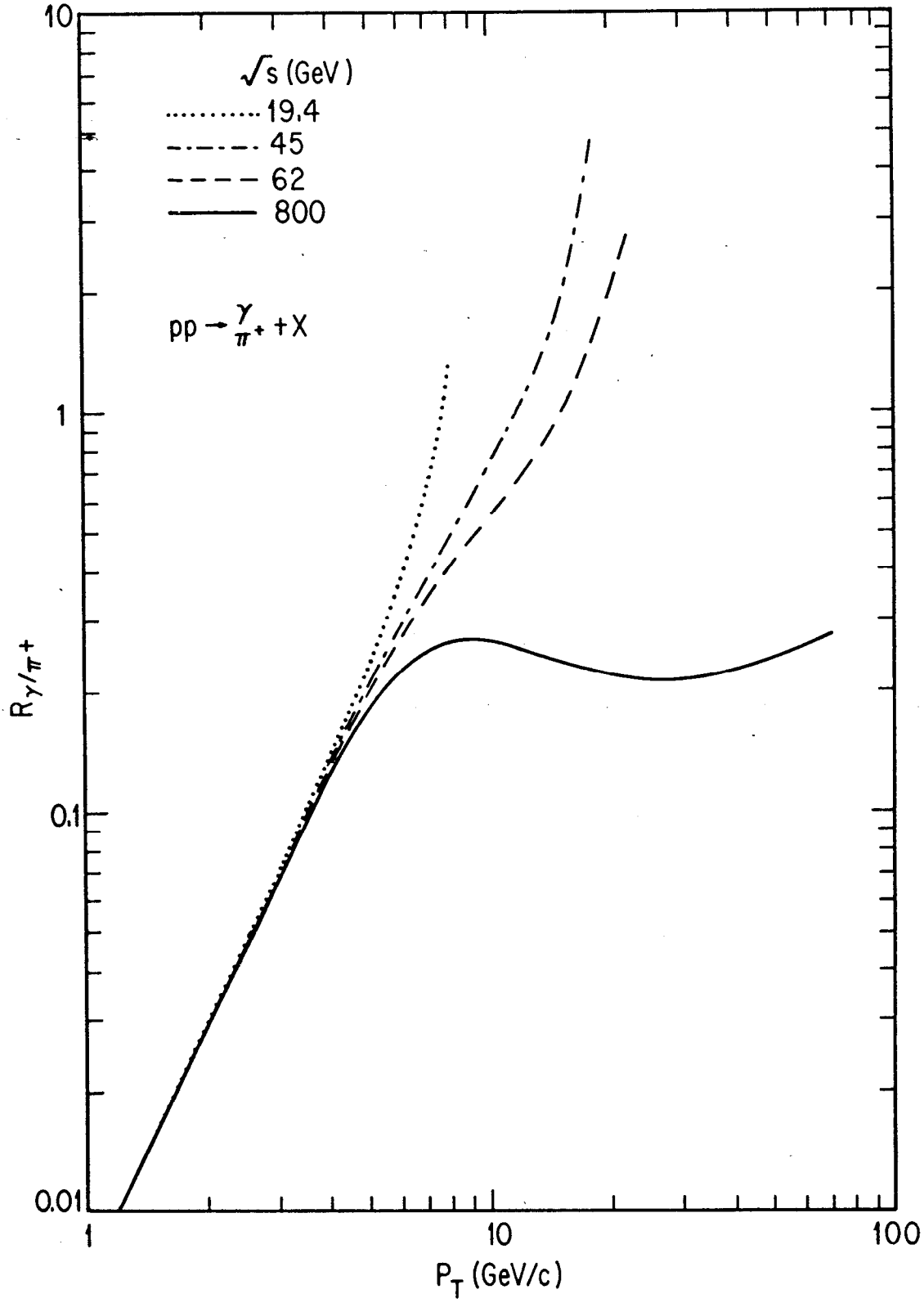

Fig. 6

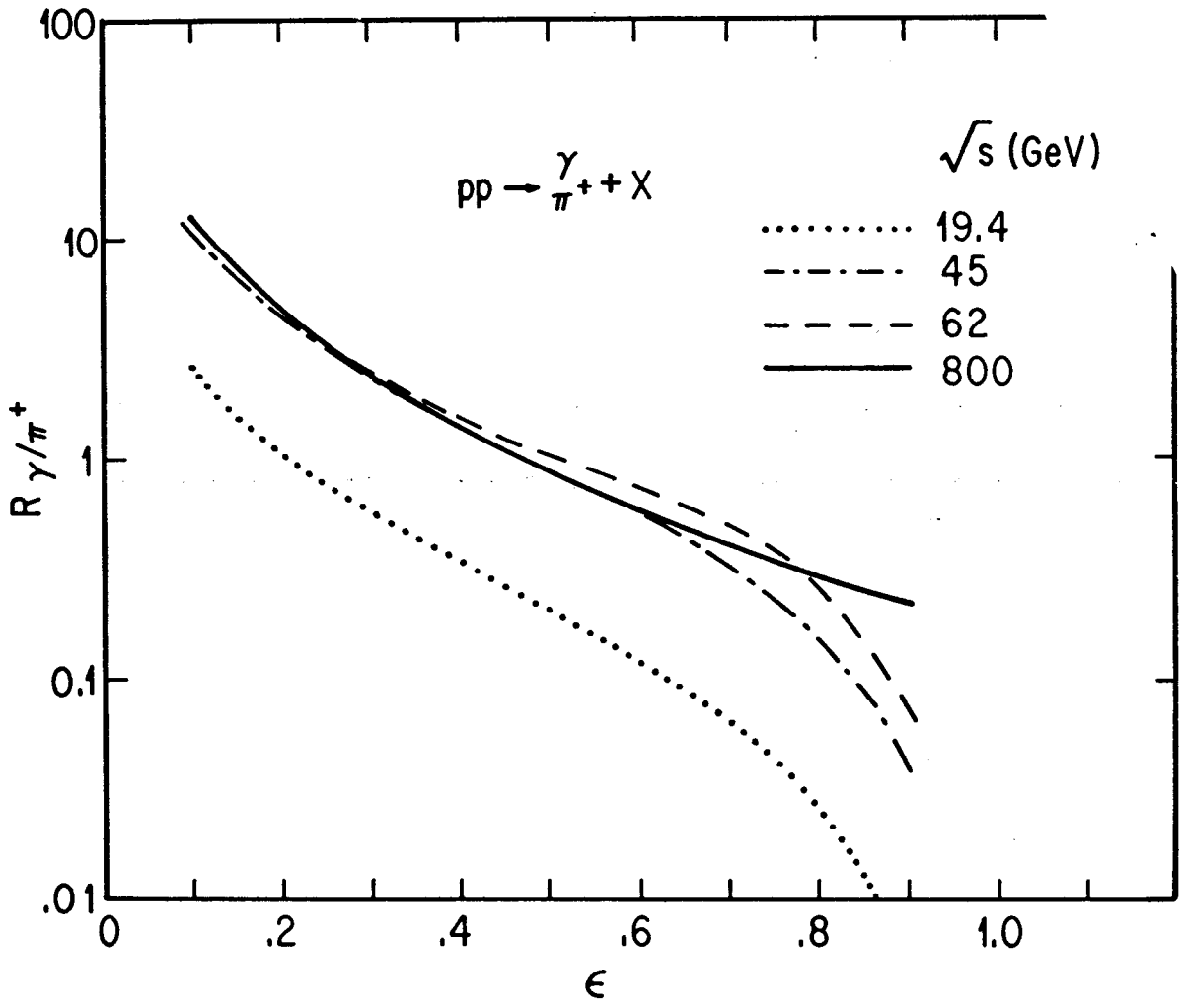
100
10
1
0.1
.01
0
.2
.4
.6
.8
1.0
R_{γ/π^+}
ϵ
$pp \rightarrow \frac{\gamma}{\pi^+} + X$
$\sqrt{s}$ (GeV)
19.4
45
62
800

Fig. 7

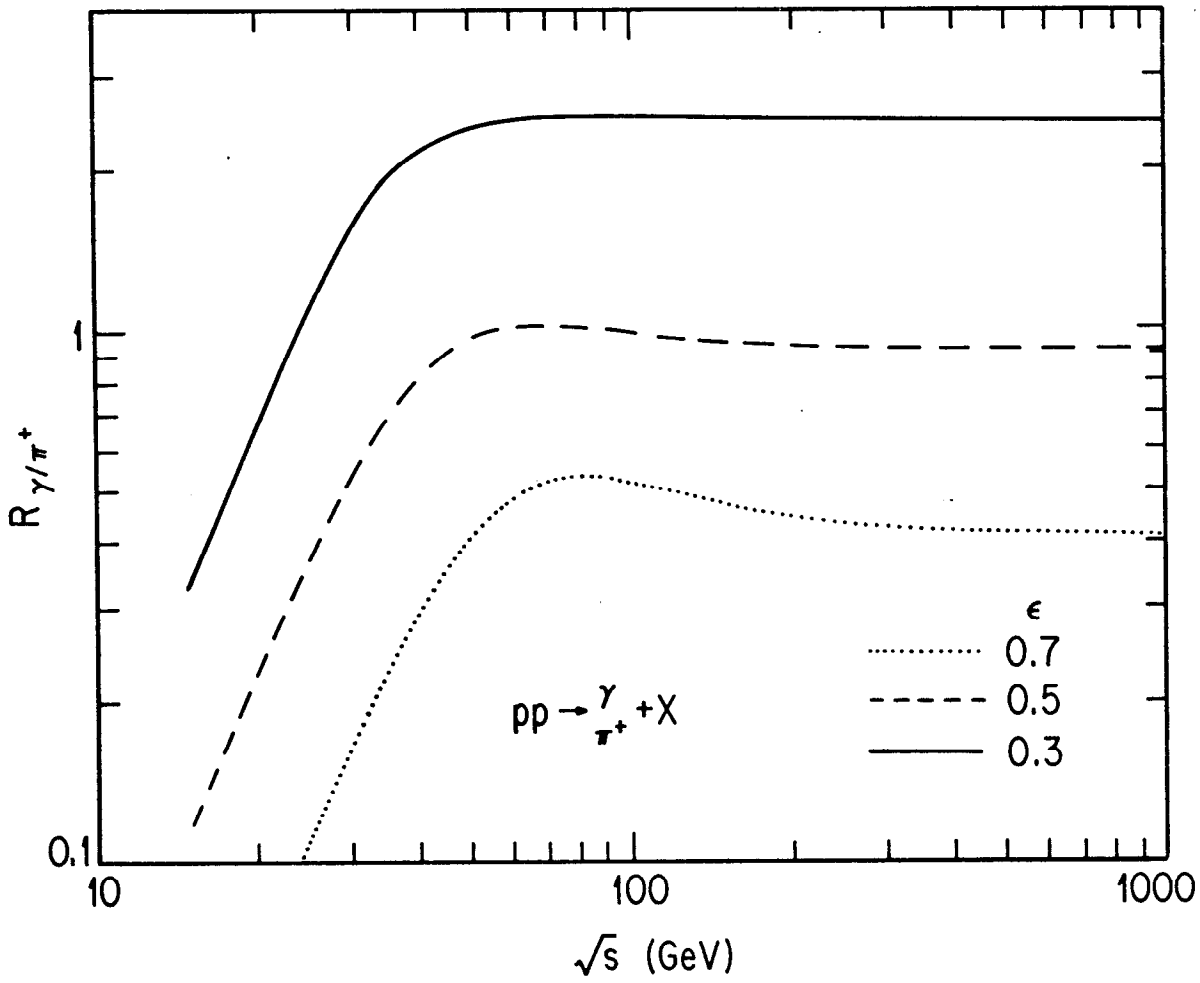
R_{γ/π^+}
1
0.1
10
100
1000
$\sqrt{s}$ (GeV)
$pp \to \frac{\gamma}{\pi^+} + X$
ϵ
0.7
0.5
0.3

Fig. 8

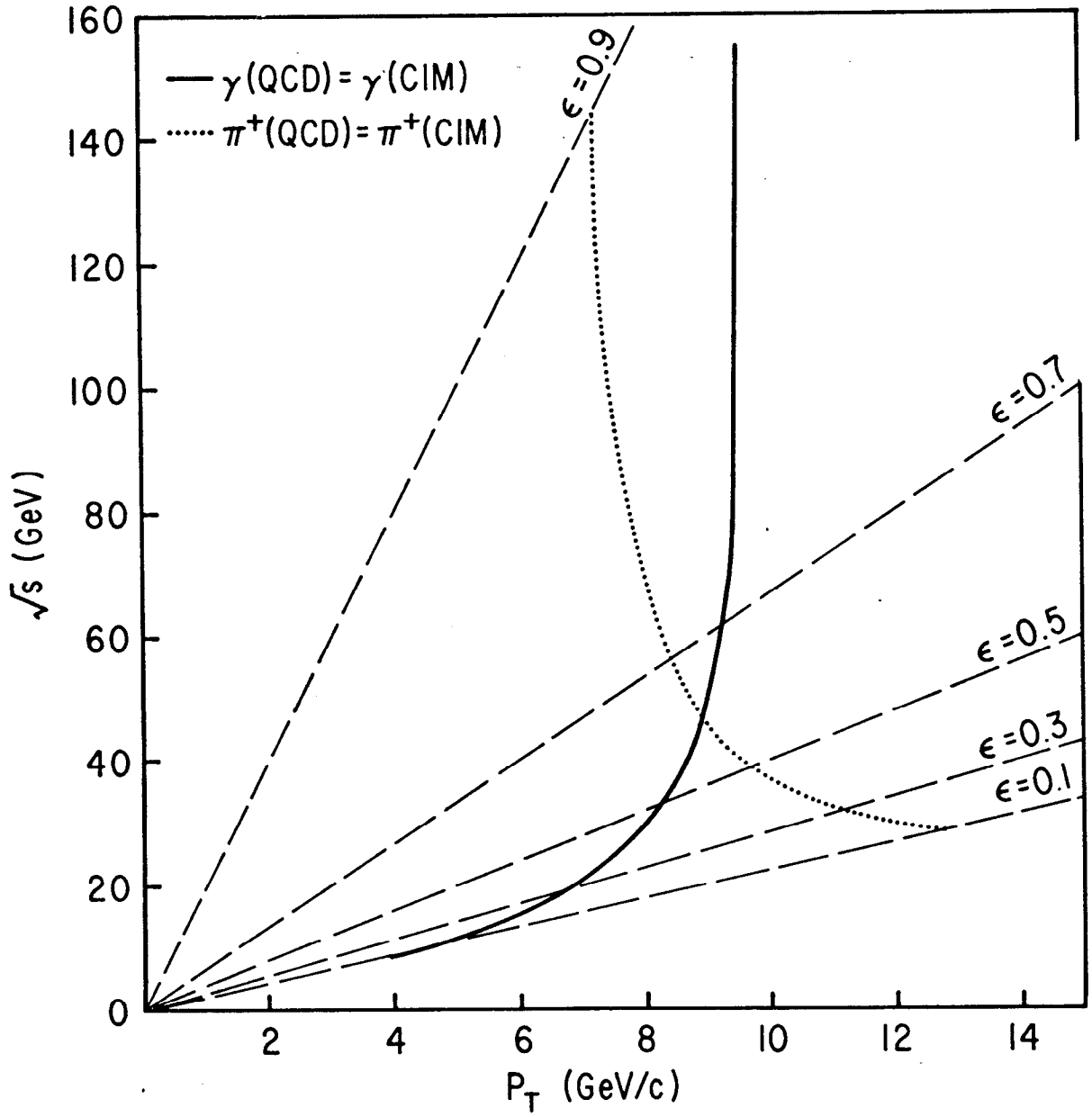
160
140
120
100
80
60
40
20
0
$\sqrt{s}$ (GeV)
2
4
6
8
10
12
14
P_T (GeV/c)
γ(QCD) = γ(CIM)
π^+(QCD) = π^+(CIM)
ϵ=0.9
ϵ=0.7
ϵ=0.5
ϵ=0.3
ϵ=0.1

Fig. 9

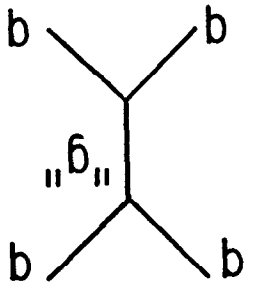

Fig. 10

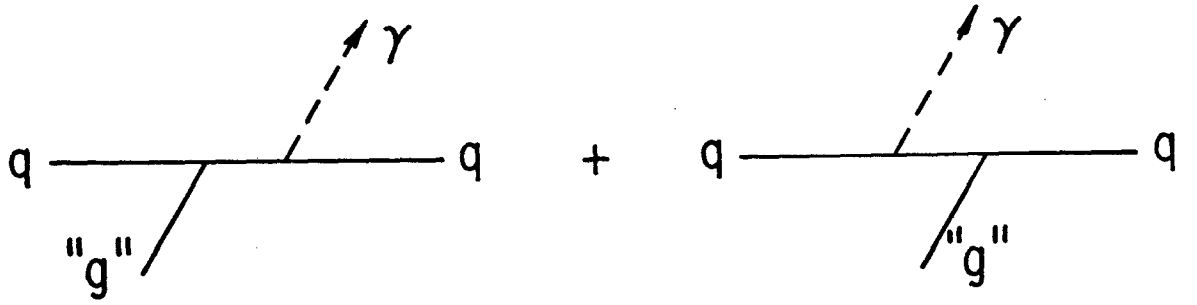

Fig. 11